UNIVERSIDAD NACIONAL DE COLOMBIA

Markerless Analysis of Gait Patterns in the Parkinson's Disease

Juan Carlos León Alcázar

Universidad Nacional de Colombia
Facultad de Ingeniería, Departamento de Ingeniería de Sistemas e Industrial
Bogota, Colombia
2012

Markerless Analysis of Gait Patterns in the Parkinson's Disease

Juan Carlos León Alcázar

Tesis presentada como requisito parcial para optar al título de:
Magister en Ingeniería de Sistemas y Computación

Director:
Ph.D. MD. Eduardo Romero Castro

Línea de Investigación:
Procesamiento de Imágenes, Análisis de Movimiento Humano
Grupo de Investigación:
Cim&Lab

Universidad Nacional de Colombia
Facultad de Ingeniería, Departamento de Ingeniería de Sistemas e Industrial
Bogota, Colombia
2012

“I think we’ve got enough information now, don’t you?”
”All we have is one ’fact’ you made up“
“ That’s plenty. By the time we add an introduction, a few illustrations and a conclusion, it will look like a graduate thesis.”
Calvin & Hobbes

Acknowledgments

First, I would like to express my sincere thanks to my advisor Prof. Eduardo Romero for his valuable guidance, and support in so many projects along these years of work. It was just a great experience to work with him and with all the people that have gathered around his projects. Also I would like to thank the other members of the "Motion Analysis Group" Fabio and Christian for all the ideas we shared and all the help they provided during the elaboration of this thesis.

Finally I would also like to thank my family for the support and patience they have shown all this years.

Abstract

In the clinical praxis Gait Analysis constitutes one of the key tools for the diagnose and follow up of some pathologies. The conventional approach includes the approximation of the skeleton by the placement and detection of a set of markers, this procedure has some relevant drawbacks and can be better approached by a markerless strategy, where the dynamics of the body are estimated without the use of any artifact. The main goal of this thesis is to present some markerless approaches that allow the characterization of the human gait. For the analysis pathological gait, we focus on the Parkinson's Disease, a neurodegenerative disorder whose symptoms results in difficulty to perform complex motor task among them walking.
Keywords: Gait Analysis, Parkinson's Disease, Background Subtraction, Tracking

Resumen

En la practica clínica el análisis de marcha es una de las herramientas más importantes para el diagnostico y seguimiento de algunas patologías. Este análisis incluye la aproximación del esqueleto mediante marcadores colocados sobre el paciente. Debido a que este procedimiento tiene algunas desventajas, se han desarrollado aproximaciones sin marcadores para el análisis de marcha, estas intentan capturar la dinámica del movimiento del paciente prescindiendo de cualquier artefacto. El objetivo principal de esta tesis es presentar algunas aproximaciones sin marcadores al análisis para marcha patológica. La patología que analizamos es la enfermedad de parkinson, un desorden neurodegenerativo cuyos síntomas resultan en la creciente dificultad para realizar tareas motoras complejas entre ellas la marcha.
Palabras Clave: Análisis de marcha, Enfermedad de Parkinson, Substracción de Fondo, Tracking

Contents

. Acknowledgments **v**

. Abstract **vi**

1. Introduction **2**

2. Gait Analysis & The Parkinson's Disease **3**
2.1. Clinical Gait Analysis . . . 3
2.1.1. Markerless Gait Analysis . . . 5
2.2. Parkinson's Disease . . . 6
2.2.1. Diagnose and Follow up of the Parkinson's Disease . . . 7
2.2.2. Altered Gait Patterns on The Parkinson's Disease . . . 8
2.3. Conclusions . . . 9

3. Biomarkers & The Parkinson's Disease **10**
3.1. Biomarkers . . . 10
3.2. Biomarkers in the Parkinson's disease . . . 11
3.2.1. Biomarkers for the Parkinson's disease . . . 12
3.2.2. Conclusions . . . 12

4. Background Subtraction **14**
4.1. $\Sigma - \Delta$ Estimation & Background Subtraction . . . 16
4.1.1. $\Sigma - \Delta$ modulation for Background Subtraction . . . 17
4.1.2. Multiresolution $\Sigma - \Delta$ Background Subtraction . . . 18
4.2. Conclusions . . . 18

5. A Robust Background Subtraction Algorithm using the Σ - Δ Estimation **19**

6. Classification of Pathological Gait Markerless Patterns **26**

7. Gesture Recognition of Pathological Gait Markerless **36**

8. Model Based Analysis of Gait Patterns **41**
8.1. Human Gait Models . . . 42

8.2. Filtering 42
8.2.1. Bayesian Filtering 43
8.2.2. The Annealed Particle Filtering 44
8.3. Matching 46
8.3.1. Matching Algorithm 46
8.4. Pathological Gait Characterization 47
8.4.1. Results 48
8.5. Conclusions 49

9. Conclusions and Future Work **51**

A. Derivation of relevant Particle Filter Equations **53**

. Bibliography **54**

1. Introduction

Gait analysis is one of the key tools for the diagnose and follow up of the Parkinson's disease, as the motor symptoms of the disease largely alter the normal gait patterns of the patients; This analysis is usually performed by the detection of a set of markers in a video sequence of the patient's gait, this classic approach has some relevant limitations related with the approximation of the skeleton by the markers positions.

This thesis analyzes the use of the human gait as biomarker for the Parkinson's disease under a markerless approach, were gait patterns are estimated by the detection and tracking of the human body along a video sequence. The first chapters present the motivations and key tools for the development of this work. Chapter 2 introduces the classical and the markerless gait analysis techniques along with the main reasons to use the gait for the clinical diagnose and follow up of the Parkinson's disease. Chapter 3 provides a brief overview of the use biomarkers for the assessment of a pathology and highlights the importance of biomarkers in the Parkinson's disease. Chapter 3 analyzes common strategies for background subtraction, a key tool in markerless analysis which provides information on the dynamics of the human body in a video sequence.

Chapters 5 , 6, 7 and 8 contain the results of this thesis, with the first 3 presented as published on international conferences. Chapter 5 presents an extension of the Σ - Δ estimation for background subtraction that improves the detection of lower limbs. Chapters 6, 7 introduce markeless model-less strategies for characterization of gait patterns, where the first one is based on Motion History Images, and the second uses a sumarization of a visual descriptor of the frames. Chapter 8 presents a final strategy for characterization of gait patterns built upon a mechanical model of the lower limbs.

2. Gait Analysis & The Parkinson's Disease

A gait analysis consist in a systematic quantification, follow up and interpretation of the temporal sequence of movements that characterize human locomotion. This procedure requires the collection of kinematic and kinetic data that describe displacements, angles and forces on the lower limbs and their joints during the gait cycle. These data are obtained from three primary information sources: video, Electromyography (EMG) and force platforms[14, 5].
Video capture of a gait sequence is one of the common methods used to gather data in gait analysis; it attempts to establish the position and alignments of the lower limbs from the image sequence, usually by simplifying the limbs into articulated figures that approximate the underlying skeleton[3].
Although the estimation of the limb position and alignment, obtained from the video, provides a useful description of the gait kinematics, it contributes little information about the muscular activation or the forces generated at the lower limbs. Therefore techniques like EMG are used to complement the video data gathered in the gait laboratory. EMG measures the electrical potential generated by muscle cells during muscular activity by means of surface or needle electrodes, thereby providing insight on muscle activations[54]. Further information comes out from the analysis of the foot ground reaction forces. This data come from force platforms located along the patient's path, recording the forces and moments along the x,y and z axes and the approximate coordinates of the center of pressure[56].
Other sources of information as pressure mats, gyroscopes, accelerometers, stroboscopic imagery and instrumented shoes are also used, however these are less common. The set of tools and techniques dedicated to collect gait data is what is currently known as the gait laboratory.

2.1. Clinical Gait Analysis

Gait analysis is a topic of interest in many fields: animation, sports science, and surveillance; In the clinical field it has special relevance as the distortion of gait patterns is an early clinical manifestation of many diseases, among others diabetes, brain palsy, Parkinson's Disease and some musculoskeletal disorders. For these pathologies, gait analysis can be used to complement other clinical tests either for the identification of a pathology or to assess the effectiveness of an intervention, with the side gain that it this a not an invasive procedure[41].

While gait analysis can be performed on a pure observational form i.e. without recording or measuring any kind of data, the conclusions of such analysis are subjective and based exclusively on the clinician's expertise and the discovered gait disturbances can only be recorded in a descriptive way[31]. Therefore measuring instruments (as those mentioned in the later section) are used to objectively asses the patient's gait patterns, in this scenario two types of gait analysis can be differentiated:

Unassisted Gait Analysis In the unassisted gait analysis the diagnosis is still limited by the ability of the clinician to handle large amounts of data, generated by the selected measurement instruments and still relies on his/her expertise with the biomechanics of the observed pathology or pathologies[57], however the gait deviations are objectively measured and are available for further examination or follow up.

Assisted gait analysis The assisted gait analysis, applies mathematical methods for data analysis in order to support the clinician's diagnose and decision making, reducing the time spent in analysis, its subjectivity and the probability of a wrong diagnose[41, 57].

In the praxis, the most used source of information for the gait analysis is the kinematic description of the body parts involved in the gait, i.e. the angles, angular velocity, location, displacements and speed of the lower limbs. Therefore *marker based analysis* is the most common technique for gait analysis[59]. In this setup a set of artifacts that can easily be recognized in a video sequence (markers) are placed upon some specific anatomical locations, one or several gait sequences of the patient are then recorded in video Finally, the locations of the markers are used to approximate the skeleton along the video sequence.

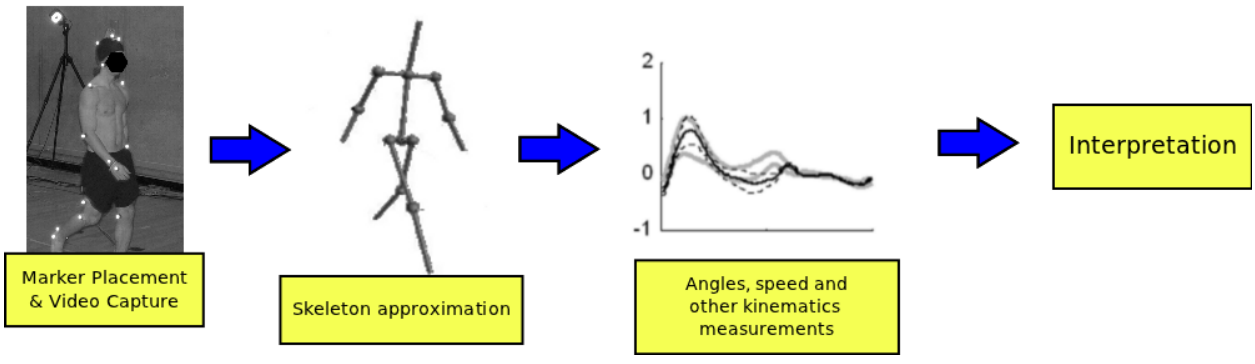

Figure 2-1.: Classical marker based gait analysis workflow

In spite of being a common technique, there are some important drawbacks to marker based gait analysis that limit its accuracy and effectiveness, largely related with a proper location of the markers, possible displacements and alteration of the natural gait gesture in such analysis.

Smooth tissues displace and rotate relative to the underlying bones, specially near the joints. Such movement can alter the correspondence between the marker or array of markers and the anatomical region of interest[1], limiting the accuracy of the estimated kinematics. This error affects every measurement that relies on artifacts placed on the skin of the patient and usually derives in body segments of variable size, this displacement is a well known source of error named "Skin Movement Artifact" [3, 29, 32].
The location of the markers can be a relevant source of error, as inaccurate placements of the markers yield poor estimations of the underlying skeleton. These errors usually propagate, e.g. a wrong location of the Hip joint center will affect the estimation of the femur alignment with the center of the knee joint[52]. This error can further accentuate the anatomical variability of pathological subjects, for example a diabetic foot. This is the main source of error in modern gait analysis[53, 5].
Finally, marker based strategies commonly ignore the environment where the patient is moving. Under these conditions, accurate estimation of key events of the gait cycle as the "toe off" and "heel strike", are challenging, and usually require of complementary information obtained from force platforms or EMG[53].
These difficulties can be avoided if instead of estimating the underlying skeleton from a set of markers, the natural gestures of the movement are captured and then analyzed, an approach known as the *markerless analysis*.

2.1.1. Markerless Gait Analysis

In recent years the quick evolution of sensors for motion capture have enabled alternatives to the marker based analysis, among them the markerless analysis, where the goal is no longer to identify a set of markers and infer the arrangement of the skeleton, but to recognize and interpret the human movement using only the shape and dynamics of the human body[59]. Unlike marker based analysis, there is not an established protocol or methodology for markerless gait analysis, however most approaches share 5 general aspects shown in figure **2-2**:

Model The model is an apriori knowledge of the observed motion, it is usually a mechanical or biomechanical approximation. The model initialization is the configuration of every possible parameter e.g. forces, sizes, degrees of freedom, that might change according to the observed gait in the video i.e models are adapted to the dynamics of normal or pathological gait.

Visual Features With an initialized model, visual features that are considered relevant for the movement analysis are extracted from each frame of the video sequence. Although a broad range of features can be extracted from an image, the selected visual features are commonly low level features, e.g edges, optical flow, foreground pixels or blobs,

[1] When using an array of markers to locate a single region, the relative positions of the markers is altered due to skin movement, introducing additional noise to the measures

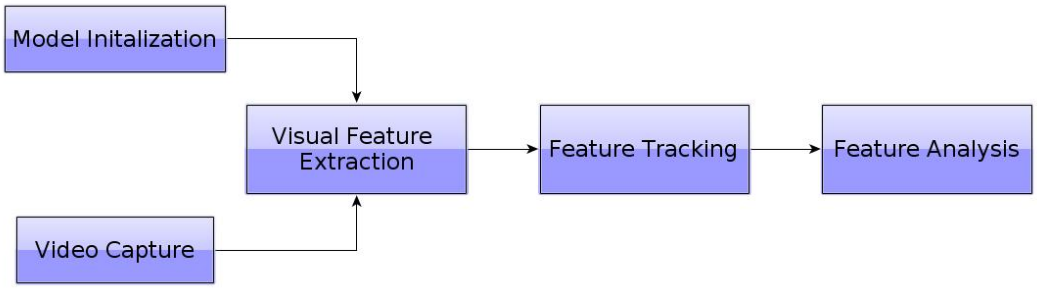

Figure 2-2.: Markerless gait analysis workflow

because such features can be easily associated with the movement of the human body in the video[39].

Tracking Single image features provide little information of the human motion in the video sequence; However, their progression along the video provides useful information on the dynamics of the gait. This progression can be approximated by a tracking step, where the goal is to establish a temporal correspondence for the extracted features of the video, such that a given feature at time t can be related to itself at time $t-n$ $(n > 0)$[39]. If the tracked features can be associated to the human pose, its is possible to establish the position and relative alignment of relevant body parts through the video, thus allowing the estimation of temporal trajectories.
The model, if any, is used at this step as the prior that enables the estimation of the human pose by Bayesian estimation[].

Feature Analysis Finally the feature analysis step extracts high level information from the tracked features, normally by classifying the motion into a set of classes as normal or pathological gait[39].

As mentioned earlier, there is not an established methodology for markerless gait analysis. Therefore not every approach uses all the described steps, there are approaches without models which relay exclusively on the extracted features for learning and recognition. Some approaches might also work without features tracking, in which case some strategy is used instead to keep the history of the features.

2.2. Parkinson's Disease

Parkinson's disease (PD) is a neurodegenerative disorder characterized by the progressive death of selected neuron populations, specially the dopaminergic neurons, located within the substantia nigra pars compacta. This results in a loss of the neurotransmitter dopamine, which generates a series of motor disabilities characteristic of the PD[27, 43].

The major motor signs and symptoms of PD include *tremor*, usually at a frequency between 4 and 6 Hz and prominent at the end of the extremities; *bradykinesia* or slowness of movement, which is related to the difficulties in planning, initiating and executing movements; *rigidity* to passive movement of the limbs and *postural deformities*, which include flexed neck, elbows and knees and flexed trunk posture[24]. The advance of these symptoms results in progressive difficulty to perform complex motor task such as writing, speaking and walking[10].
PD is, worldwide, the second most common neurodegenerative disorder, surpassed only by Alzheimer's disease, Yet it is rare in persons under the age of 40, its prevalence is estimated at 1% for the population between 60 and 69 years of age and nearly 3% among 80 year people and older[42, 30].
After an average of 5 years of disease, most of patients also develop non-motor symptoms, among them: cognitive decline, depression and autonomic failure as well as pain and sensory symptoms, after 15 years from diagnosis, more than 70% of patients would have died and about half of those surviving, require nursing-home care[46]. This marked impact on the quality of life along with the treatment costs, which have been estimated up to €8000 (direct costs) and €7000 (indirect cost) per patient a year[2], the absence of a cure for the disease[2] and the aging of the population, project the PD as one of the most relevant health concerns in the years to come.

2.2.1. Diagnose and Follow up of the Parkinson's Disease

A reliable and easily applicable diagnostic test or marker to confirm the presence or advance of PD is not yet available[30]. The only way to confirm a PD diagnosis is assessing the presence of Lewy Bodies in the substantia nigra, however, given the location of the substantia nigra in the midbrain (see figure **2-3**), this procedure can only be performed during an autopsy[50].
In the clinical praxis, diagnosis and assessment of the advance of PD can be difficult, specially for the early stages, as it lies on clinical observation and interpretation of motor features as those already described in section 2.2 [23, 24]. This analysis strongly depends on the expertise of the specialist. After an initial diagnose, long term follow up of the patient is required to revisit and improve the initial diagnosis, and to assess the progression of the disease, based mostly on the appearance of additional symptoms and responsiveness to levodopa therapy[30].
The progress of the PD, is commonly evauated with the UPDRS[3] (Unified Parkinson's Disease Rating Scale), designed to capture diverse signs of the PD, as the diminished cognitive abilities, difficulty while performing everyday tasks and rigidity, among others[48].

[2]Currently, there is no cure for the PD, treatment is limited to relief from the symptoms and its effectiveness usually declines with the advance of the disease [43].

[3]Other scales as "Hoehn & Yahr" and "Schwab and England Activities of Daily Living" are also used to asses the progress of the PD, however the most common is UPDRS

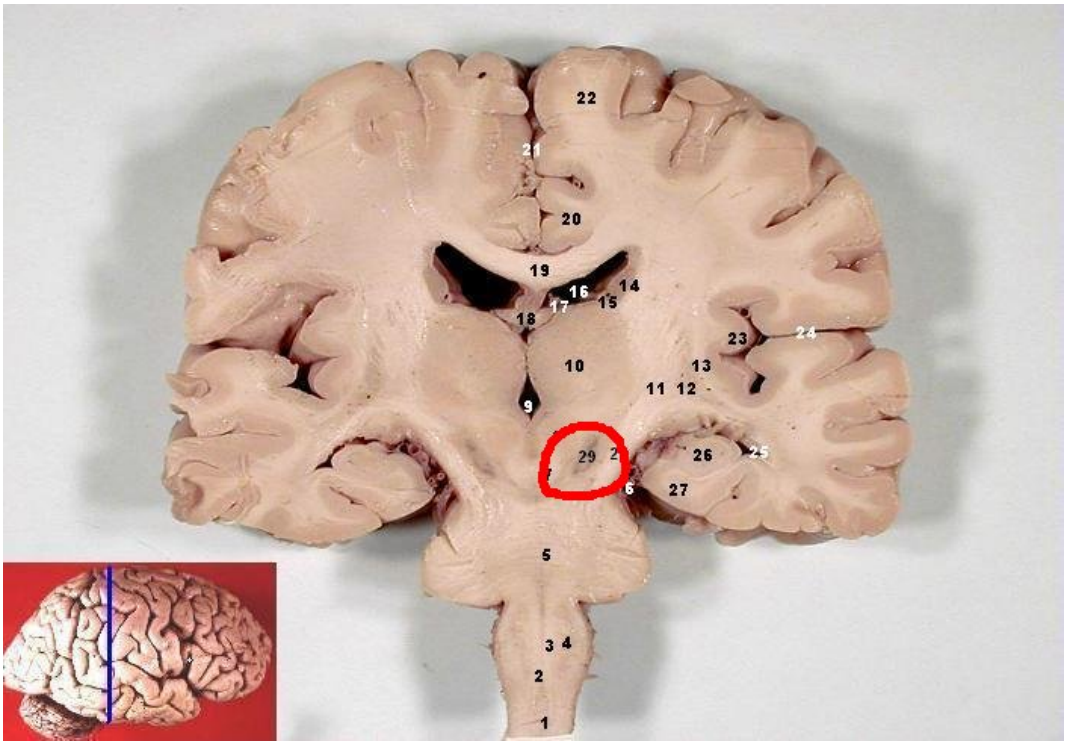

Figure 2-3.: Location of the substantia nigra (29).

Even with this protocol and rating scales, diagnosis and advance assessment of PD can still be subjective and inaccurate, studies have shown that between 10% and 25% of PD diagnoses can not be confirmed at the autopsy, specially those made at the early or intermediate stages [12, 28, 26].

2.2.2. Altered Gait Patterns on The Parkinson's Disease

As mentioned in section 2.2, PD results in the difficulty to perform complex motor tasks, thus altered gait patterns are among the most relevant signs for diagnose and follow up of PD[13]. There are several studies that relate some of the PD rating scales with quantitative evaluations that can be performed in the gait laboratory[48].
Excluding severe cases, patients with PD can walk straightforwardly without external assistance[36], however their limbs move at a slower rate and with a smaller amplitude than those of healthy people on the same age group. They also show difficulties while performing simultaneous motor or cognitive tasks as walking and speaking, or changing the walk direction, finally PD patients usually have difficulties to move in environments with obstacles or restricted spaces[8].
The natural straight-line gait gestures under semi-controled conditions, as those of a gait laboratory, are affected in the PD, specifically patients with the disease show:

- Diminished or absent arm swing.
- Reduced trunk rotation.
- Lean forward stance.
- Low amplitude movements at the hips, knee and ankles.
- Short stride, with reduced step cadence.
- Reduced foot clearance.

A patient wit PD walks at an average speed of 40 to 60 meters per minute in straight line, far under the average of 70-90 meters per minute of a healthy person. The average number of steps per minute is between 100 and 110 per minute, similar to the average of a healthy subject, however the amplitude of the steps is reduced for persons with PD, between 0.4 and 0.9 meters compared with the normal stride length, between 1.2 y 1.5 meters. Finally the amount of time of gait cycle that the PD patient spends in double stance is larger, compared with healthy subjects: for the former it is over 35% and for the later it is between 20% and 30% [35, 51, 36, 25, 44].
Given the set of well known and measurable patterns, gait analysis constitutes, in the clinical praxis, one of the key tools for the diagnose and follow up of PD.

2.3. Conclusions

Markerless gait analysis is an alternative to marker-based analysis, where the difficulties associated with the marker location and possible displacements are no longer an issue. The markerless analysis provides a better source of information as it allows the capture of the natural gesture and dynamics of the gait without oversimplifying the human figure to the underlying skelleton.

The Parkinson's Disease affects the motor capabilities, changing the characteristic straight line gait patterns. Such alterations can be studied in a gait laboratory, as a result, walking patterns can be established for individuals with Parkinson's Disease, which differ from those of healthy subjects and vary as the disease advances.

As the markerless gait analysis allows detection and follow up of the gait dynamics of an individual, it should be possible to discover and measure the characteristic straight line walking patterns of the Parkinson's Disease with a markerless framework and establish the difference between those patterns and normal gait patterns.

3. Biomarkers & The Parkinson's Disease

In recent years, new technologies and tools have been developed to support clinical diagnose, decision making, treatment, disease monitoring and drug discovery and development. These techniques relay often on the identification of biological characteristics that serve as an indicator of a particular disease or physiological state and the development of tools to analyze them. Such indicators are known as biomarkers and are commonly used to monitor and predict the health of an individual or population[20].

3.1. Biomarkers

Following the National Institutes of Health definitions working group, a Biomarker is "a characteristic that is objectively measured and evaluated as an indicator of normal biological process, pathogenic process, or pharmacologic responses to a therapeutic intervention"[21]. Thus biomarkers are commonly used in clinical studies, where the efficacy of an intervention must be evaluated in an quantitative and unbiased manner and for disease detection and quantification[49].

There are three essential properties for a biological characteristic to be considered as a valid biomarker; First there must exist a *biological plausibility* between the biological process and the biomarker, that is, a link between the process and the measures obtained from the biomarker exists; Second the biomarker should be *sensitive and specific*, when used for disease detection the biomarker should have the ability to identify positive and negative results with low error rate, when used for drug test or disease quantification, the effects of the treatment should be reflected on the measures of the biomarker; Third a biomarker should be *standardized*, it must be reliable over time, and between subjects and laboratories. There are other desirable properties for a biomarker as non invasiveness and simple utilization these are however not required[49, 20].

Based on this properties there are 3 criteria to evaluate the the validity of a biomarker[20]:

Criterion validity Measures the correlation of the biomarker with the gold standard of a given pathology, it also measures the ability of the biomarker to reflect the effectiveness of an intervention.

Construct validity Refers to the existence of scientific evidence that demonstrates the link between the clinical outcome and the biomarker.

Face validity Face validity refers to the biological plausibility of the biomarker

It is clear from the later definitions and properties that there must exists a relationship between the biological process and the characteristic selected as biomarker, there are however two ways this relationship can be established: the biomarker can either be an indicator of the actual pathological process or of its clinical phenotype. The first option is preferred as those biomarkers can be used in the very early stages of a pathology, and are usually more accurate than biomarkers associated to a clinical phenotype, as erroneous results could be obtained due to other pathologies that generate a similar phenotype[37].
Biomarkers associated with the clinical phenotype are only preferred if it is not possible to obtain information of the pathological process or to asses the effectiveness of an intervention specifically designed to handle the symptoms of a pathology[37].
Finally, there are two common approaches to construct biomarkers which are closely associated to the relationship between the biomarker and the biological process, a *bottom up* approach uses the knowledge of the underlying pathological process for the construction of the biomarker, but as stated above this is not always possible, thus *top down* approaches build biomarkers based on the related clinical phenotype of a given pathology[20, 37].

3.2. Biomarkers in the Parkinson's disease

A biomarker can be used to assess the existence of a pathology or the effectiveness of an intervention. The Parkinson's Disease (PD) and its treatments are not an exception, accurate information about the ongoing disease process can be used to direct treatments, however, as stated in chapter 2, PD results from the death of neurons located in a region of the brain which can only be directly analyzed postmortem. This lack of information on the actual disease process, along with clinical signs that fluctuate over time, limit the existing biomarkers to those targeted at the pathological phenotype and make it difficult to monitor PD in an accurate and unbiased manner[37], hence there are currently two main goals for the development of biomarkers for the PD:
Diagnosis improvement. Novel biomarkers could improve the reliability of PD diagnose, as mentioned in chapter 2 between 10% to 25% of PD diagnoses can not be confirmed, such errors can be largely attributed to the existence of syndromes that have similar signs (tremor, hypokinesia, rigidity, and postural instability) without the characteristic neurodegenerative process of PD[]. Novel biomarkers are also key for the early diagnosis of PD, it is known that the characteristics signs of PD appear after a loss of 50% to 60% of the dopaminergic neuron cells[27, 37] a process which lasts around 5 years []; An accurate diagnose during this stage could lead to better treatments, capable of delaying the onset of important motor and non-motor symptoms.

Parkinson's disease progression & follow up. After a PD diagnose, it is important to have a quantitative indicator of the advance of the disease at the moment of diagnosis and during treatment to assess its effectiveness. Biomarkers and their progression are an objective source of information to make such assessments, avoiding the subjectivity of an analysis based exclusively on the clinician expertise and the possible inter-observer variability of some rating scales [37].

3.2.1. Biomarkers for the Parkinson's disease

As it is not possible to analyze the subtantia nigra directly, several biomarkers have been developed for the analysis of the clinical phenotype of the PD, here is a brief list of the most commonly used biomarkers for the diagnose and follow up of the disease:

Imaging Brain Imaging is one of the most interesting biomarkers for the PD, as it allows to gather information from the substantia nigra, thus image markers might be able to detect the early pathological process of the PD. Some image modalities as Positron Emission Tomography and Single Photon Emission Computed Tomography have been used to discover signs of the cell loss that characterizes PD, however there is still not a reliable biomarker for PD based on brain imaging[37].

Clinical testing Besides the motor signs described in section 2.2, there are other clinical markers related to the PD. Studies have shown that affected olfactory discrimination, sleep disorders, retinal degeneration, gastrointestinal dysfunction and depression among others signs are associated to the PD[23]. Still among these biomarkers, motor disorders are those that are best documented and are the easier to assess objectively.

Biochemical The analysis of markers in the cerebrospinal fluid or plasma is a known aid for the diagnosis of neurological disorders, similar approaches have been tried for the PD. Although some biomarkers based on protein and oxidative stress have been studied, there is still not a reliable diagnostic biomarker directly related to the degenerative process characteristic of PD[23, 37].

Genetic While genetic markers can not asses the existence or advance of PD, they are useful to estimate the risk of PD for a given individual or population. Although some genes leading to Mendelian inheritance of PD and parkinsonism have been identified, it still remains unclear how to use a genetic test as a reliable predictor of PD[23].

3.2.2. Conclusions

Currently the construction of biomarkers for the PD is limited to top down approaches as the underlaying pathological process can only be directly evaluated during an autopsy. Among those PD biomarkers targeted at the pathological phenotype, the analysis of gait patterns

is one of the most convenient as there are well known gait patterns for the normal gait, that gets largely altered during the different stages of the disease.

4. Background Subtraction

The initial step of our approach requires the segmentation of the human silhouette in a gait sequence, the nature of the captures in the gait laboratory i.e. static camera, semi-controlled illumination conditions and a single person in movement, allows to perform this segmentation by means of a background subtraction (BS) method, which detects and follows moving objects along videos sequences through the identification of pixels with large temporal changes.

Figure 4-1.: Sample gait laboratory sequence, under controlled illumination conditions and static background the human figure can be segmented by highlighting pixels with large temporal changes

BS methods assume that a scene is composed of a fixed background and moving objects, which have different color distributions[6], therefore most BS methods classify pixels as either background or foreground based on the difference between the pixels and some model of the background, this can be stated as:

$$B_t(x,y) = \begin{cases} 1 & \text{if } d(I_t(x,y), M_t(x,y)) > \tau_{x,y,t} \\ 0 & \text{otherwise} \end{cases} \tag{4-1}$$

Where $I_t(x,y)$ are the pixels of the frame at time t, $M_t(x,y)$ is the model established up to time t, $d(I_t, M_t)$ is a function that measures the difference between the current frame and the

current model, $\tau_{x,y,t}$ is a bound that can be updated for each frame or pixel and $B_t(x, y)$ is a binary image with intensity 1 if the pixel is classified as foreground and 0 for background[6]. In BS problems the construction of a good model of the background is critical. A a naive approach would use a reference image of the background without any object and classify as foreground any intensity difference found on the video sequence. Provided that such reference background can be obtained, this naive approach would only work on controlled environments, as any illumination change, misalignment of the capture device, change in the background, noise during the capture or processing of the image sequence will affect the results[47]. Clearly this approach can be improved with a dynamically updated background model.

Running Average. The easiest way to build a dynamic M_t is to calculate it as running average over I_t:

$$M_{t+1} = (1 - \alpha)M_t + \alpha I_t \tag{4-2}$$

Where α is constant with values in the range $[0, 1]$, that controls the balance between the stability of the update and its speed, for simplicity and efficiency M_0 is, most times, set to I_0[58]. Some authors replace the running average by the median calculated on a time window $[t, n],\ 0 < n < t$, as its is more robust to noise at the expense of some computational complexity[45].

Gaussian model. The later approach is easy to implement and is favored if there are little computational resources available e.g. the BS algorithm is implemented on an embedded device. However, it is sensible to noise and to the value of the parameter α, it also builds an average of the scene including moving objects, which is undesired. This can be better approached by explicitly modeling the color distribution of the background. One of the most used models is a Gaussian distribution adjusted to the history of per-pixel intensities up to time t, or in a time window $[t, n],\ 0 < n < t$, thus modeling the background at time t with a matrix of means $\mu_{x,y,t}$ and covariances $\Sigma_{x,y,t}$, thereby changing the background subtraction problem into an outlier detection problem[6].

Gaussian mixtures. While the latter approach yields better approximations of M_t, some scenes can not be properly modeled by a single Gaussian distribution, i.e illumination or parts of the background might change over time, therefore some BS methods employ a Gaussian mixture to model the background, in such models, M_t is given by a set of means and covariances $\{\mu_{x,y,t,1}, \Sigma_{x,y,t,1}\}, \{\mu_{x,y,t,2}, \Sigma_{x,y,t,2}\} \ldots \{\mu_{x,y,t,n}, \Sigma_{x,y,t,n}\}$ and the labeling of a pixel as foreground or background is based on the probability:

$$P(B_{x,y,t}) = \sum_i w_i \eta(\mu_{x,y,t,i}, \Sigma_{x,y,t,i}) \tag{4-3}$$

Where w_i is an assigned weight to the i-th Gaussian distribution used to model the background[45], again the BS problem is converted into an outlier detection problem.

Kernel Density Estimation. Non parametric models have also been used for the estimation of M_t, one of the most common is the Kernel Density Estimation, where the probability function that models the background over a window of N frames:

$$P(B_t) = \frac{1}{N} \sum_{k=t-N}^{t-1} K_h(I_t - I_k) \tag{4-4}$$

Where K is a kernel function with bandwidth h, in these approaches a pixel is considered foreground if it is unlikely to be generated from the estimated distribution i.e $P(B_t)$ is low[38].

4.1. $\Sigma - \Delta$ Estimation & Background Subtraction

Among the BS techniques, the $\Sigma - \Delta$ operator represents a family of background subtraction methods based on the $\Sigma - \Delta$ modulation, well known for their computational efficiency and capability to work without any prior knowledge of the scene.

The $\Sigma - \Delta$ modulation oversamples a signal at higher rates than the specified by the Nyquist theorem, increasing the correlation between adjacent frames, thus the quantization error power spreads over a wide range of frequencies, while the signal power remains within the signal band, allowing a good separation of the input signal from the quantization noise[9].

The block diagram of a first order $\Sigma - \Delta$ modulator is shown in figure **4-2**, the Σ block is an integrator, and the Δ block is a quantizer. As the signal is multiplied by the output of the pulse generator, $y(n)$ is the integral of the differences between the information carrying signal $x(n)$ and the modulator's output encoded as a 1-bit signal. This output can be reconstructed by means of a low pass filter[9].

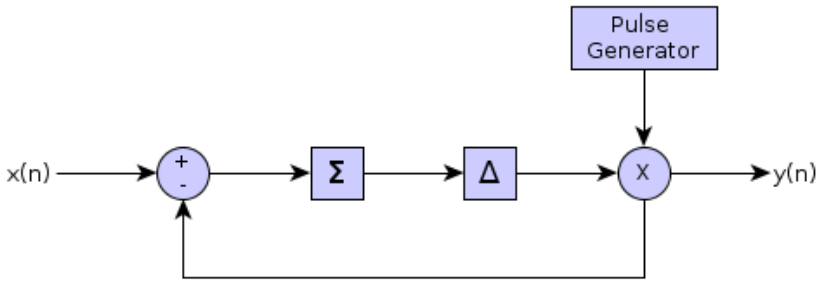

Figure 4-2.: A first order $\Sigma - \Delta$ modulator

4.1.1. $\Sigma - \Delta$ modulation for Background Subtraction

When applied in BS tasks the $\Sigma - \Delta$ modulator, dynamically updates a background tracker $M_t(x, y)$, by comparing each image $I_t(x, y)$ with $M_t(x, y)$, using a simple updating rule: If $I_t(x, y)$ is greater (lower) than $M_t(x, y)$, then a positive increase (decrease) Δ is performed so that steady variations on the background are tracked[33]. A detailed description of the $\Sigma - \Delta$ modulation for Background subtraction can be found in algorithm 1[1].

Algorithm 1 Basic $\Sigma - \Delta$ Algorithm

```
Initialization: M_0(x) = I_0(x)
for each Frame t do
    M_t(x) = M_{t-1}(x) + sgn(I_t(x) − M_{t-1}(x))
    Δ_t(x) = |M_t(x) − I_t(x)|
end for
Initialize: V_0(x) = Δ_t(x)
for each Frame t do
    for each pixel x such that Δ_t(x) ≠ 0 do
        V_t(x) = V_{t-1}(x) + sgn(N × Δ_t(x) − V_{t-1}(x))
        if Δ_t(x) < V_t(x) then
            D_t(x) = 0
        else
            D_t(x) = 1
        end if
    end for
end for
```

In spite of its simplicity $\Sigma - \Delta$ operator has several interesting properties as background tracker. First, the background estimation can be interpreted as a simulation of a digital conversion of a time-varying analog signal using $\Sigma - \Delta$ modulation. Second, the $\Sigma - \Delta$ modulation works better for signals whose absolute time-derivative is less than unity, that is when the change on the signal is "small" between samples, common on gait laboratory sequences. Third, the filter computes the time-variance of the pixels which is a measure of temporal activity of the pixels that allows the detection of state changes on the pixel, from "moving" to "stationary" or vice-versa. Fourth, the $\Sigma - \Delta$ uses a nonlinear approximation for statistics M_t and V_t as both are updated by ± 1 on each iteration, whereas a linear approach would be equivalent to the moving average. Fifth, it processes each pixel independently and is based on simple integer additions and comparisons therefore it demands little computational resources and is suitable for massive parallel implementations[33, 22].

[1] The algorithm is written for a 1 dimensional signal, however the $\Sigma - \Delta$ BS operates pixelwise hence the described algorithm can be applied independently to each pixel of the image

4.1.2. Multiresolution $\Sigma - \Delta$ Background Subtraction

Although the $\Sigma - \Delta$ Background Subtraction is one of the most effective yet efficient BS methods, the method still has some drawbacks, the main one is that it relies on the intensity of the pixel as its unique descriptor; A more robust approach that uses a multiresolution strategy to characterize the pixel was proposed during the elaboration of this thesis. The paper detailing this extension to the $\Sigma - \Delta$ BS can be found on Chapter 5

4.2. Conclusions

Background subtraction techniques can be used as the first step in a markerless approach for gait analysis, as they highlight the human silhouette in each of the frames of the video sequence, without the need of artifacts placed upon the patient or any prior knowledge of the scene.

Among the many Background subtraction techniques, the $\Sigma - \Delta$ operator represents a family of efficient background trackers that can be extended and applied to the segmentation of the human silhouette in gait analysis.

5. A Robust Background Subtraction Algorithm using the Σ - Δ Estimation

As presented on the "International Joint Conference on Computer Vision, Imaging and Computer Graphics Theory and Applications" VISAPP 2011, february 2012

A ROBUST BACKGROUND SUBTRACTION ALGORITHM USING THE A $\Sigma - \Delta$ ESTIMATION

Applied to the Visual Analysis of Human Motion

Juan Carlos León [1], Fabio Martínez [1] and Eduardo Romero[1]
[1]*CimaLab, Universidad Nacional de Colombia, Bogotá, Colombia*

{*jcleonal, fmartinezc, edromero*}*@unal.edu.co*

Keywords: Background Subtraction, Motion analysis, $\Sigma\Delta$ estimation

Abstract: This paper introduces a novel method for segmenting the human silhouette in video sequences, based on a local version of the classical $\Sigma\Delta$ filter. A main difference of our approach is that the filter is not pixel-wise oriented, but rather region wise adjusted by using scaled estimations of both the pixel intensity and the horizontal (vertical) gradient, i.e., a multiresolution wavelet decomposition using Haar functions. The classical $\Sigma\Delta$ filter is independently applied to each component of the obtained feature vector, previously normalized and a single scalar value is associated to the pixel by averaging the feature vector components. The background is estimated by setting a threshold in a histogram constructed with these integrated values, attempting to maximize the interclass variance. This strategy was evaluated in a set of 6 videos, taken from the Human Eva data set. Results show that the proposed algorithm provides a better segmentation of the human silhouette, specially in the limbs, which are critical for human movement analysis

1 Introduction

Visual analysis of human motion implies the detection, follow up and characterization of relevant patterns in a sequence of images. Usually the main features to detect are the position and alignment of the human body parts (human pose). While visual markers can be employed for this task(Kirtley, 2005), the result is usually a simplified model of the human body. Most detection methods use a background estimation as preprocessing step, attempting to eliminate pixels with no temporal change.

Background subtraction methods use a sequence of images ($\{I_i\}_{i=1:t}$) to build a model of the static scene (M_i), and establish a rule to set a pixel value in I_i as either background or foreground.

A main contribution of the present paper was to adapt the classical $\Sigma\Delta$ pixel wise estimation to a local version of the filter, which is much more robust to local variations and tracks better the image object edges. The basic idea was to approach the pixel information with a multiresolution decomposition, conserving the edge features in the gradient estimations while the low frequency characteristics regularize the numerical difference, i.e., a classical wavelet approximation. The obtained Haar coefficients are used independently in a classical $\Sigma - \Delta$ estimation, averaged and used to construct an histogram in which an optimal threshold maximizes the interclass variance. This paper is organized as follows: Section 2 introduces the $\Sigma - \Delta$ operator, and the proposed extension, section 3 demonstrates the effectiveness of the method, finally section 4 concludes with a discussion of the proposed method and possible future works.

2 Materials and Methods

Among the background subtraction techniques, the $\Sigma - \Delta$ operator represents a family of background subtraction methods, well known for their computational efficiency and capability to work without any prior knowledge of the scene, even in no controlled illumination conditions.

While this operator offers a baseline for background subtraction in human movement analysis, it is still limited regarding its accuracy and robustness to noise. As observed in figure 1, relevant parts of the human figure, as the shins and lower arms, are missing. Noise is present on the image, especially while the model converges to a good approximation of the

background.

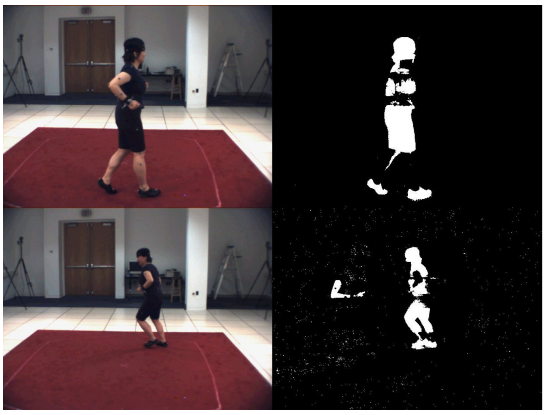

Figure 1: Output of the Basic $\Sigma - \Delta$ Algorithm for a sequence of the Human Eva Dataset

These limitations can be attributed to the selected pixel descriptors in a single frame, i.e. the regular $\Sigma - \Delta$ uses a single pixel intensity. This may be better approached by introducing local information. The present investigation proposes an extension of the $\Sigma - \Delta$ background subtraction algorithm, focusing on region features rather than on pixel intensity.

2.1 The $\Sigma - \Delta$ Operator

The non linear operator $\Sigma\Delta$ increases the correlation between adjacent frames by oversampling a signal at higher rates than the specified by the Nyquist theorem. This operator dynamically updates a background model $M_t(x)$, by comparing each image $I_t(x)$ with the current background model $M_t(x)$, using a simple updating rule: If $I_t(x)$ is greater (lower) than $M_t(x)$, then a positive increase (decrease) Δ is performed. The absolute difference $|I_t(x) - M_t(x)|$ is used to compute an estimate of the per pixel variance $V_t(x)$, and based on this estimate, pixels are classified as either foreground or background (Manzanera and Richefeu, 2007).

2.2 Region Features

As stated above, a main limitation of the $\Sigma\Delta$ background subtraction is that it operates exclusively over the intensity values of a pixel through an image sequence I_t, restricting thereby the accuracy and robustness of the background estimation process. We approached herein this problem by projecting each frame I_t into a multiresolution space. Unlike a classical multiresolution decomposition, the different image scales are not herein obtained by a simple downsampling of the original image, but rather by a local

Algorithm 1 Basic $\Sigma - \Delta$ Algorithm

```
Initialization: M_0(x) = I_0(x)
for each Frame t do
    M_t(x) = M_{t-1}(x) + sgn(I_t(x) - M_{t-1}(x))
    Δ_t(x) = |M_t(x) - I_t(x)|
end for
Initialize: V_0(x) = Δ_t(x)
for each Frame t do
    for each pixel x such that Δ_t(x) ≠ 0 do
        V_t(x) = V_{t-1}(x) + sgn(N × Δ_t(x) - V_{t-1}(x))
        if Δ_t(x) < V_t(x) then
            D_t(x) = 0
        else
            D_t(x) = 1
        end if
    end for
end for
```

pixel neighbourhood smoothing upon which a block Haar wavelet analysis is carried out. In our scheme we use a set of features calculated from the Speeded Up Local Descriptor (SULD), proposed by Zhao et al. (Zhao et al., 2009) and now on used as a pixel descriptor. The low frequency is computed as the average of a neighbourhood centred at the pixel, while the high frequency is calculated by firstly averaging a spatial shifted version of the previously used neighbourhood, and then differences between the up-down (left-right) shifted neighbourhoods are stored. The calculated values are closely related to the gradients and therefore to the edges along the x and y axes, as seen in figure 2. Each image pixel is associated to a feature vector with three components containing an average of the different scale pixel descriptors, i.e., the neighbourhood sizes. This allows to systematically remove finer details or high-frequency information from an image, achieving a compact description of the most relevant information which is usually preserved through multiple scales. Therefore, the first step of our approach was to build, for each pixel, a multidimensional feature vector containing the local first order information.

These features are calculated for each of the n channels of the image and used as input of the $\Sigma - \Delta$ algorithm, after normalization, yielding a $3n$ dimensional descriptor for each pixel.

2.2.1 Efficient Feature Calculation

The two first features are calculated as the difference of the sum of pixel intensities within two shifted boxes, either vertically or horizontally. This can be efficiently computed using the summed area table

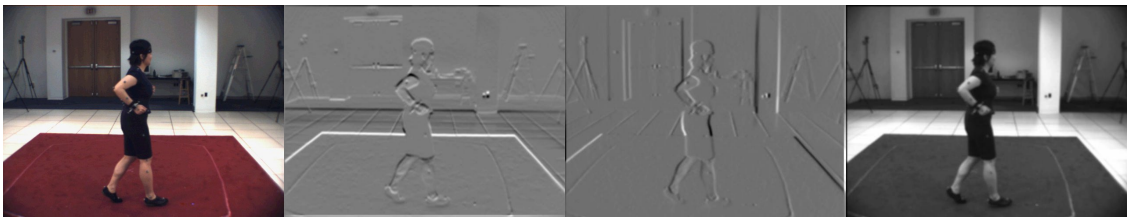

Figure 2: Descriptors, from left to right: original image, vertically and horizontally filter response maps , sum of values in region

known as the integral image (Viola and Jones, 2001), case in which an image (ii) replaces a pixel value (i) with the sum of the intensity of every pixel located above and before it, formally:

$$ii(x,y) = \sum_{x' \leq x} \sum_{y' \leq y} i(x',y') \tag{1}$$

The use of the integral image optimizes calculation of the region intensity sum and read as:

$$\sum_{j<x' \leq k} \sum_{m<y' \leq n} i(x',y') = ii(j,m) + ii(k,n) - ii(k,m) - ii(j,n) \tag{2}$$

2.3 Foreground Classification Criteria

The basic $\Sigma - \Delta$ algorithm uses a simple classification criterion: the last pixel intensity variation ($\Delta_t(x)$) is compared with an estimation of the cumulated variance ($V_t(x)$), if the result is positive then the pixel is marked as foreground, otherwise it is considered as background. This metric does not fit our multidimensional representation: while the mentioned criterion may be applied to each feature, another metric must be built to produce a final decision from the obtained set of per-feature decisions. To overcome these limitations, we propose a multidimensional metric that associates the feature vector to a single scalar value, obtained by integrating on every feature component and shifting from the $[-1,1]$ to the $[0,2]$ interval. Each image pixel is assigned then to a particular (P_t) value, an estimate of the regional changes, the higher (lower) a P_t value is the more (less) likely the corresponding pixel in I_t is a foreground pixel. A change is then defined if the history of regional changes is smaller than the change reported by the current local analysis. For achieving so, we exploit the characteristics of the histogram's waveform of P_t, where background pixels are near 0 and their number is significantly larger than the foreground pixels. Hence we build two classes, one with a small (large) number of bins which contains most (few) scene pixels: the background (foreground). We are interested in a value that maximizes the intra-class variance by comparing the variances of the two previously defined classes. For doing so, let us suppose that we have k different bins, starting from an initial bin, a class is composed of a set of bins that are progressively increased by including new bins into the class. The algorithm includes new bins in each class by running forward (backward) over the histogram, starting from 0 and k for the background and foreground classes, respectively. The goal is to stop when the variance of the two classes is alike and its magnitude is maximum. We search then for a bin (γ) where the consecutive per group variances are close and large in magnitude for both classes as follows: for a histogram with k bins let

$$\alpha_i = var(bin_0 ....bin_{i-1}) - var(bin_0 ....bin_i) \tag{3}$$

the consecutive variance of a background estimation composed of bins 0 to i, likewise let

$$\beta_i = var(bin_k, ..., bin_{i+1}) - var(bin_k, ..., bin_i) \tag{4}$$

the difference of variances for the foreground group up to bin i. A set of candidate bins Γ_i is stablished with

$$i \in \Gamma \iff \frac{\alpha_i}{\beta_i} \approx -1 \tag{5}$$

Among all the candidates in Γ_i we choose γ as as the one with the larger magnitude in the variance differences i.e.

$$\gamma = \max_{\Gamma_i} |\alpha_i \beta_i| \tag{6}$$

2.4 Dataset Description

Validation was carried out with a subset of the Human Eva Dataset (Sigal et al., 2010), composed from 3 different subjects, each captured from 2 different cameras for a total of 6 sequences. Each sequence was manually labeled, as frame n has almost the same foreground and background of frame $n \pm 1$ labeling was done only once per 10 frames, additionally the labeling only started at the 40th frame this accounts for an initial estimation of the background (stabilization) of both algorithms.

3 Evaluation and Results

There are well know metrics to evaluate the performance of a binary classification, however most of these metrics assume that there is approximately a balanced quantity of elements in the classes. In this dataset the foreground usually amounts to less than the 10% of pixels in the image, hence we choose the true positive rate (TPR), and the Matthews Correlation Coefficient (MCC), the former is independent of the class distribution, while the later is designed to measure the quality of the classification even with unbalanced classes.

During the evaluation of the algorithm it was clear that scales (box sizes) larger than 11 were not appropriate for the segmentation of relative small objects in movement (like the hands and forearms), also the body boundaries are not properly located. Therefore we first seek for a combination of scales between 1 and 11 that provides the best results, for this particular dataset the selected scales were 1,3 and 5. The results are summarized in tables 1 & 2.

Sequence	Regular $\Sigma - \Delta$ TPR	Proposed $\Sigma - \Delta$ TPR
1	37.94%	67.46%
2	55.73%	68.95%
3	31.61%	69.23%
4	57.63%	73.25%
5	48.62%	71.94 %
6	65.86%	78.05%

Table 1: True positive Rate

Sequence	Regular $\Sigma - \Delta$ MCC	Proposed $\Sigma - \Delta$ MCC
1	0.557	0.683
2	0.707	0.678
3	0.524	0.721
4	0.725	0.731
5	0.656	0.713
6	0.767	0.774

Table 2: Matthews Correlation Coefficient

The TPR of the proposed method outperforms the regular $\Sigma\Delta$ in every test sequence, this can be attributed to the better detection of the limbs in motion, specially the shins and forearms (see figure 6).

An interesting feature of the proposed algorithm can be analysed with table 1, our method offers a large improvement for sequences 1, 3 and 5 (30.06% average) however the improvement for sequences 2, 4 and 6 is smaller (13.71% average). This is related to the background of the sequences, on the first group the background has several objects of different colors on it i.e. it contains borders, the background of the later group has a single color and is nearly flat (see figure 3). The absence of borders lowers the effectiveness of the proposed algorithm as the input information for the $\Sigma\Delta$ comes mainly from the intensities of neighbouring pixels.

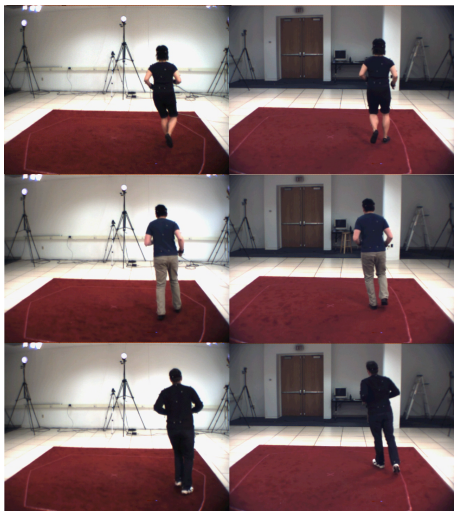

Figure 3: Sequences 2,4,6 on the left side, sequences 1, 3, 5 on the right side

While the TPR shows a significant improvement of our algorithm over the regular $\Sigma\Delta$, the MCC shows cases where there is not a significant improvement over the base algorithm. This can be attributed to the nature of the dataset, where the moving object (human body) is present and in motion on the first frames, this generates ghosts on every scene for both algorithms, these ghosts last longer in our algorithm thus increasing the amount of False Positives on the first frames, drawing down the average MCC for the sequence.

This can be seen in figures 4 and 7, while the first frames show an MCC for the proposed algorithm under the MCC of the regular sigma delta, on the next frames (when the ghost starts to fade) the MCC of our algorithm is better, even in the second sequence, where out algorithm had an average MCC under the regular $\Sigma\Delta$ (fig. 4).

Again the nature of the background seems to have influence on how long the ghosts last, scenes 1, 3 and 5. have ghosts that last shorter than the ghosts in scenes 2,4,6.

3.1 Performance

As stated on section 2, one of the main features of the $\Sigma\Delta$ Background subtraction is its computational efficiency, therefore we briefly analyze the performance penalty of the multiscale features and the new classification criterion.

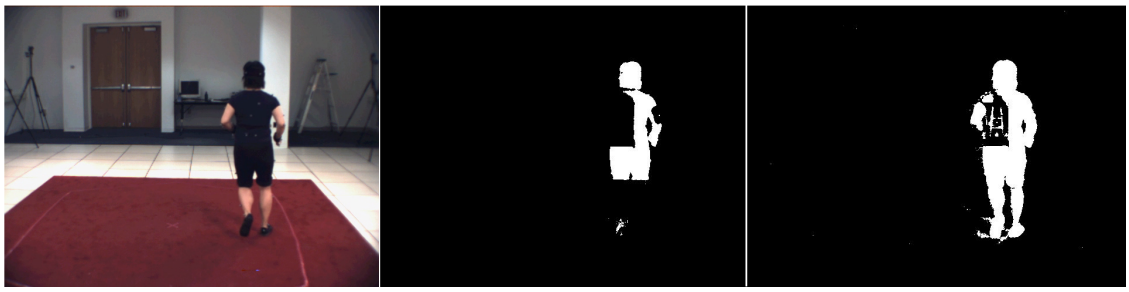

Figure 6: Results of the segmentation, from left to right, Original image, regular ΣΔ segmentation, proposed algorithm segmentation

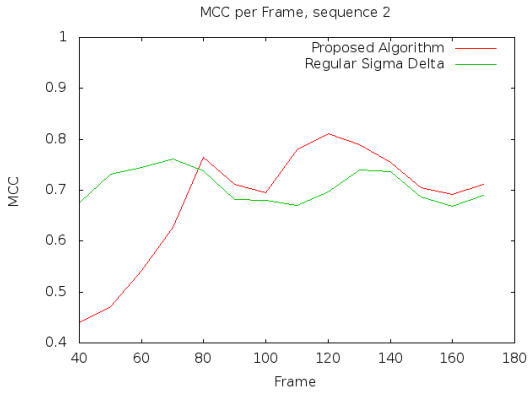

Figure 4: Comparison of the per frame MCC for sequence 2

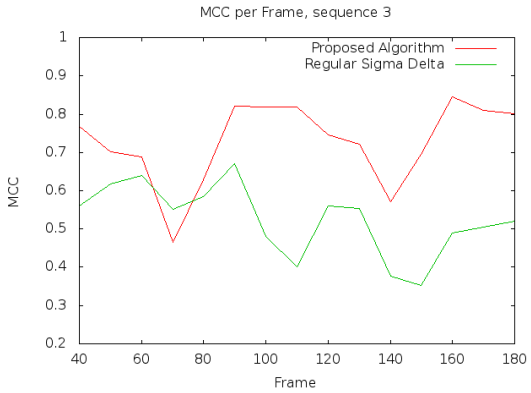

Figure 5: Comparison of the per frame MCC for sequence 3

A GNU Octave implementation of both algorithms was tested on an core i7 processor at 3.3 Ghz, on this set up the average the regular ΣΔ can process 6.72 million pixels per second. The speed of the proposed extension depends on the number of scales used for the analysis, we calculated the average speed of the proposed algorithm for a number of scales between 1 and 9, the results are summarized on table 3

Number of scales	Average pixels per second (millions)
1	1.61
2	1.31
3	1.06
4	0.89
5	0.77

Table 3: Proposed algorithm processed pixels per second

Although the base ΣΔ is faster, when the proposed algorithm is compared with other variations of the ΣΔ operator for background subtraction proposed on the literature (Manzanera, 2007)(Lionel Lacassagne, 2009) (Richefeu and Manzanera, 2006) it shows an average performance (see figure 7).

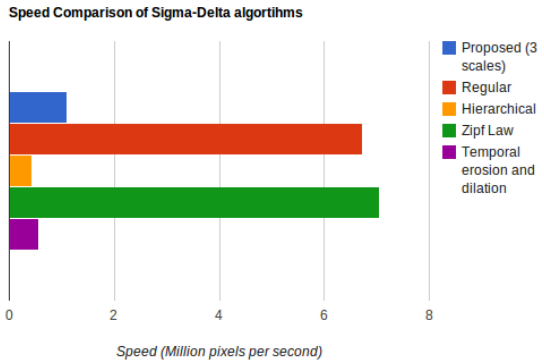

Figure 7: Speed of other ΣΔ algorithms (million pixels per second)

4 Conclusions

An novel method for segmenting the human silhouette in video sequences based on the ΣΔ background subtraction, was introduced on this paper, this

method offers a significant improvement in the background segmentation over the base ΣΔ, at the expense of computational cost.

The proposed algorithm enhances the pixel description with local features, allowing a multiscale representation of each frame, which results in an improved detection of the human body, specially at the arms and lower limbs, which is critical for tasks that require a proper description of the dynamics of the human body, as gait analysis and video surveillance.

REFERENCES

Kirtley, C. (2005). *Clinical Gait Analysis: Theory and Practice*. Churchill Livingstone.

Lionel Lacassagne, A. M. . A. D. (2009). Motion detection: Fast and robust algorithms for embedded systems. In *IEEE International Conference on Image Processing*.

Manzanera, A. (2007). Sigma-delta background subtraction and the zipf law. In *Progress in Pattern Recognition, Image Analysis and Applications*.

Manzanera, A. and Richefeu, J. (2007). A new motion detection algorithm based on [sigma]-[delta] background estimation. 28(3):320–328.

Richefeu, J. and Manzanera, A. (2006). A new hybrid differential filter for motion detection. In Wojciechowski, K., Smolka, B., Palus, H., Kozera, R., Skarbek, W., and Noakes, L., editors, *Computer Vision and Graphics*, volume 32 of *Computational Imaging and Vision*, pages 727–732. Springer Netherlands.

Sigal, L., Balan, A. O., and Black., M. J. (2010). Humaneva: Synchronized video and motion capture dataset for evaluation of articulated human motion. *International Journal of Computer Vision (IJCV)*, 87.

Viola, P. and Jones, M. (2001). Robust real-time object detection. In *International Journal of Computer Vision*.

Zhao, G., Chen, L., and Chen, G. (2009). A speeded-up local descriptor for dense stereo matching. In *Image Processing (ICIP), 2009 16th IEEE International Conference on*, pages 2101–2104.

6. Classification of Pathological Gait Markerless Patterns

As presented on the "International Seminar on Medical Information Processing and Analysis"
SIAPIM 2010, December 2010

Classification of Pathological Gait Markerless Patterns

Juan Carlos León Alcazar[b,a], Fabio Martínez[a], Eduardo Romero[a,*]

[a] *BioIngenium Research Group, National University of Colombia, Bogotá, Colombia*
[b] *Scire Foundation, Bogotá, Colombia*

Abstract

Gait patterns may be distorted in a large set of pathologies. In the clinical practice, the gait is studied using a set of measurements which allow identification of pathological disorders, thereby facilitating diagnosis, treatment and follow up. These measurements are obtained from a set of markers, carefully placed in some specific anatomical locations. This conventional procedure is obviously invasive and alters the natural movement gestures, a great drawback for diagnosis and management of the early disease stages. Instead, markerless approaches attempt to capture the very nature of the movement with practically no intervention on the movement patterns. This article introduces a novel markerless strategy for classification of normal and pathological gaits, using view-based video descriptor of the sagital trajectory, stored in a temporal summarization. The strategy was evaluated in three groups of patients: normal, musculoskeletal disorders and parkinson's disease, obtaining a sensitivity around 80 %.

Keywords: Gait analysis, Motion History Images, Support Vector Machine, markerless approach

1. Introduction

Distortion of gait patterns are the first clinical manifestation of many diseases, among others diabetes, brain palsy, cerebral vascular accidents, neuromuscular dystrophies or accident sequelae. The analysis of human gait attempts to objectively assess pathologies by following up the hidden gait dynamic variables. The set of techniques dedicated to perform this analysis is what is currently known as the gait laboratory, a modern tool devised

*Eduardo Romero. Carrera 30 45-03. Ciudad Universitaria, 3165000 ext 15025, edromero@unal.edu.co

to quantify a disease, to compare the gait with normal patterns and to efficiently perform the dynamic alignment of lower member prostheses [1, 2]. Most of this gait analysis is carried out with a set of markers, carefully placed in some specific anatomical locations. This conventional procedure is invasive and alters the natural movement gestures leading to wrong pattern measures.

On the other hand, gait dynamic patterns are by nature highly variable and can be easily contaminated with noise. In early stages, most of these diseases differ by very little from what is considered a normal pattern so that classification is a very challenging problem, even for the expert clinicians. This picture may be worsen if one considers that the basic examination tool, the markers, can move very easily or even be unobservable, contaminating the resulting measurement. These factors together lead to subjective clinical analyses with the consequent limitation in the reproduction of the clinic management of the patient [3, 4].

Ultimately, this problem has undergone a fundamental transformation since the objective is not anymore the movement reconstruction from the anatomical markers, but the accurate tracking of the movement pattern i.e. the markerless strategy. Research areas as computer vision, automatic surveillance, animation and image processing have already developed some markerless strategies for diverse applications, namely, biometric identification, abnormal motion detection, scene reconstruction and activity classification [5, 6, 7]. These methods attempt an interpretation of human movements using nothing but the shape and dynamics of the body. This article presents a precise and efficient markerless framework to identify and classify different kinds of normal and pathological movements. This approach uses as input a sagital view video of a patient walking. Every frame is processed to extract the human silhouette, with which we build a view-based video descriptors that are a temporal summarization of the motion history. Hu moments are then computed for each descriptor, a feature vector is obtained and used to classify patterns as normal or pathological using a classical Support Vector Machine strategy. Evaluation was performed on a database with 48 videos from 12 patients, with 3 types of movements: normal, musculoskeletal disorders and parkinson's disease. This paper is organized as follows: Section 'Materials and Methods' introduces the proposed markerless strategy, Section Results demonstrates the effectiveness of the method and the last section concludes with a discussion and possible future works.

2. Materials and Methods

The proposed strategy segments the silhouette and uses it to construct a gait descriptor: the motion history images(MHI). This descriptor is finally used as a feature in a classical SVM strategy. The whole method is illustrated in Figure 1.

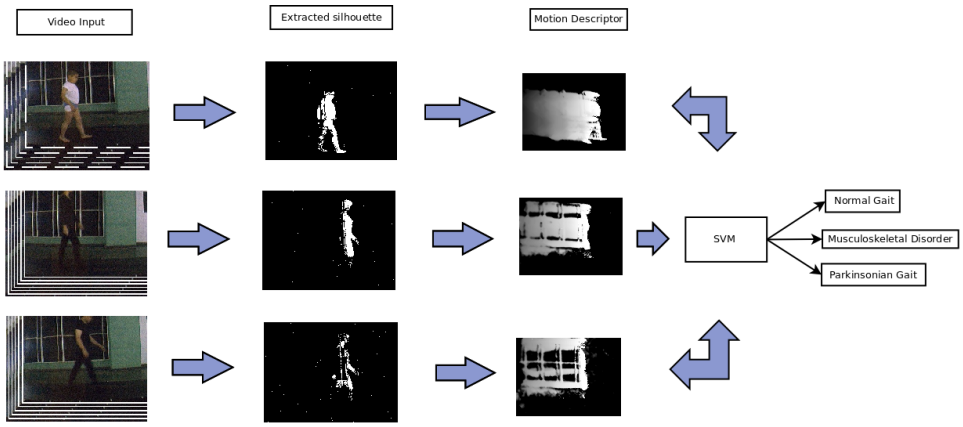

Figura 1: Markerless strategy to Classify Pathological Gait Patterns. This approach consist in a set of step: (a)walking sequence of video, (b) Silhouette extraction process using $\Sigma-\Delta$ algorithm, (c) HMI video descriptor construction, (d) classification method

2.1. Background Estimation for Silhouette Extraction

Temporal description of the patient gait patterns is central at describing structural changes. Many strategies have been proposed already, they are currently known as background estimation methods [8, 9, 10]. These methods use a sequence of images I_t and build a model of the static scene M_t. Output of the model is a Image D_t, where the background is represented by $D_t(x) = 0$ and the foreground is $D_t(x) = 1$.

Among the background estimation methods, the non linear operator $\Sigma - \Delta$ is one of the most robust. This estimator oversamples a signal at higher rates than the specified by the Nyquist theorem, increasing correlation between the adjacent frames, evaluated for each pixel [9]. The $\Sigma - \Delta$ operator behaves as a background tracker $M_t(x)$, dynamically updated by comparing each image $I_t(x)$ with the current background $M_t(x)$, using a simple updating rule: If $I_t(x)$ is greater (lower) than $M_t(x)$, then a positive increase (decrease) $+\Delta$ is performed. The implemented $\Sigma - \Delta$ algorithm is shown in 1, whose results illustrated in Figure 2(a).

(a) Walking sequence

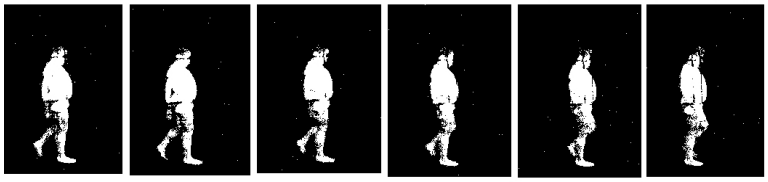

(b) Background estimation

Figura 2: Silhouette extraction estimation. (a) Walking sequence of a patient with a musculoskeletal disorder. (b) Results of the $\Sigma - \Delta$ background estimation

2.2. Video Descriptor

Once the silhouette is extracted from the video, the next step is to build a video descriptor that represents the dynamic of each walking. In our case, we use the *Motion History Image (MHI)* represented by $H_\tau(x, y, t)$ [11, 12] which describes the motion by the segmented silhouette changes $D(x, y, t) = 1$. This video descriptor consists in a sequence of consecutive silhouettes, recorded in a single image, i.e., moving pixels are brighter, as follows:

$$H_\tau(x, y, t) = \begin{cases} \tau & \text{if } D(x, y, t) = 1 \\ -max(0, H_\tau(x, y, t-1) - 1) & \\ \text{otherwise.} & \end{cases}$$

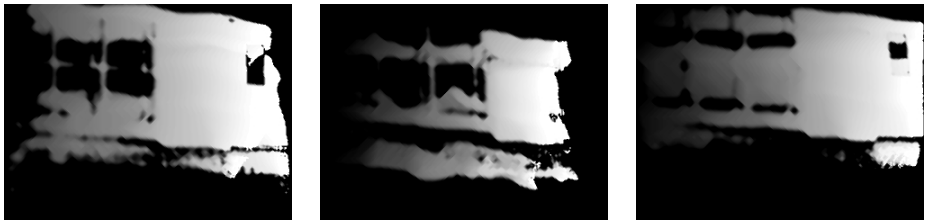

(a) (b) (c)

Figura 3: Motion History Image descriptor. (a) Normal Gait. (b)Musculo Eskeletical disease.(c) Parkinson Disease

Algorithm 1 $\Sigma - \Delta$ Algorithm

Initialization: $M_0(x) = I_0(x)$
For each Frame t
$M_t(x) = M_{t-1}(x) + sgn(I_t x - M_{t-1}(x))$

$\Delta_t(x) = |M_t(x) - I_t x|$

Initialization: $V_0(x) = \Delta_t(x)$

For each Frame t
for each pixel x such that $\Delta_t(x) \neq 0$
$V_t(x) = V_{t-1}(x) + sgn(N \times \Delta_t(x) - V_{t-1}(x))$

if $\Delta_t(x) < V_t(x)$ **then**
  $D_t(x) = 0$
else
  $D_t(x) = 1$
end if

where τ is the spatial window that defines the duration of the sagital patient motion. Figure 2.2 shows typical results for the video descriptor, in different kinds of movements. Figure 3(a) shows the typical smooth pattern of the normal walkings, while figure 3(b) shows a irregular pattern, with abrupt changes and long duration, typical of the musculoskeletal disorders [2]. Finally, figure 3(c) shows the video descriptor of a parkinson's disease walking, notice the short movement duration due to the short step length, characteristic of this kind of movement.

2.3. Gait Data

Validation was carried out with recorded sagital views, registered at the gait lab of the National University, under semi-controlled illumination conditions. The dataset consists of a set of videos captured from 12 patients, each was recorded 4 times while walking, for a total of 48 video sequences. The Dataset was divided as follows:

- 4 patients diagnosed with musculoskeletal disorders.
- 4 patients diagnosed with parkinson's disease (No depressive disorder present).

Descriptor	Samples	True Positives	True Positives Ratio
Raw Moments	33	21	63 %
Central Moments	33	24	72 %
Scale Invariant Moments	33	26	79 %
Hu Moments	33	11	66 %
Gray Descriptor	33	31	93 %

Cuadro 1: Classification results using Linear Kernel

- 4 patients with normal gait

2.4. Attributes for Classification

The Classification phase of the proposed method requires a set of attributes to be extracted from each HMI image. As image moments represent global characteristics of the image objects and provide information about various geometrical features [13], it is expected that the differences between the HMI of normal and pathological gaits can be captured by the mentioned descriptors. Therefore the first seven Raw, Central, Scale Invariant and Hu moments were selected to characterize each of the images, building a feature vector of dimension 7 for each HMI image. An additional Gray scale descriptor was included, built from a re-scaled version of the luminance channel of the original color image (it was re-scaled by a factor of 10).

3. Results

Classification was performed using a conventional machine learning method, a Support Vector Machine (SVM) [14]. The SVM was trained with a set of attribute vectors, extracted from already labeled HMI images. In this phase, two types of kernels were employed, polynomial kernels and Radial Basis Function (RBF). Parameters of the cost function, gamma (for RBF kernels) and the exponent (for polynomial kernels) were estimated using the sequential minimal optimization algorithm [15]. The Gait Dataset, with 48 videos, was split into 3 groups according to the type of gait. Each video is represented by 5 HMI and each class is represented by a total of 80 HMI images, from which 69 were selected for training and 11 images for test. The following tables summarize the obtained results.

Classification results using Linear Kernels

Classification results using RBF Kernels

Descriptor	Samples	True Positives	True Positives Ratio
Raw Moments	33	16	49 %
Central Moments	33	16	49 %
Scale Invariant Moments	33	11	33 %
Hu Moments	33	17	51 %
Gray Descriptor	33	32	96 %

Cuadro 2: Classification results using RBF Kernel

	Normal Gait		Parkinsonian Gait		Musculoskeletal	
Descriptor	Presicion	Recall	Presicion	Recall	Presicion	Recall
Raw Moments	0.635	0.91	0.429	0.27	0.429	0.27
Central Moments	0.685	1	0.75	0.545	0.75	0.545
Scale Inv. Moments	0.769	0.91	0.875	0.636	0.875	0.636
Hu Moments	0.75	0.818	0.555	0.445	0.555	0.445
Gray Descriptor	0.91	1	1	0.91	1	0.91

Cuadro 3: Recall and presions for each pathology, Linear Kernel

Recall and Precision measures using Linear Kernel

Recall and Precision measures using RBF Kernel

Tables 1 and 2 show that the re-scaled HMI is much better than the description based on moments, but at a higher computational cost. On other hand, scaled invariant and Hu moments, with a sensitivity of 80 % can be considered as appropriate for most applications, however results with HMI and a sensitivity of 96 % can even be considered for actual clinical applications.

	Normal Gait		Parkinsonian Gait		Musculoskeletal	
Descriptor	Presicion	Recall	Presicion	Recall	Presicion	Recall
Raw Moments	0.423	1	1	0.182	0.6	0.272
Central Moments	0.423	1	0.714	0.455	0.001	0
Scale Inv. Moments	0.33	1	0.001	0	0.0015	0
Hu Moments	0.473	0.818	0.001	0	0.571	0.727
Gray Descriptor	0.91	1	1	1	1	0.91

Cuadro 4: Recall and presions for each pathology, RBF Kernel

4. Conclusion

This paper presented a novel markerless method to identify and classify normal and pathological human walkings. The whole strategy consists in extracting the silhouette of the patience for each video frame and use this information for building a motion history image descriptor (HMI). Image moments are used to build a feature vector from the HMI descriptors, which is then used to classify patterns as normal or pathological using a classical Support Vector Machine strategy. The results obtained show this method could complement the conventional gait analysis and a first approximation to a markerless analysis.

Referencias

[1] C. Kirtley, Clinical Gait Analysis: Theory and Practice, Churchill Livingstone, 2005.

[2] J. Perry, J. M. Burnfield, Gait Analysis: Normal and Pathological Function, Slack, 2010.

[3] J. Kamruzzaman, R. K. Begg, Support vector machinesand other pattern recognition approaches to the diagnosis of cerebral palsy, IEEE-Trans. Biomed. Eng. 53 (2006) 2479–2490.

[4] S. Wolf, T. Loose, M. Schablowski, L. Dderlein, R. Rupp, H. J. Gerner, G. Bretthauer, R. Mikut, Automated feature assessment in instrumented gait analysis, Gait and Posture 23 (2006) 331–338.

[5] P. Turaga, R. Chellappa, V. S. Subrahmanian, O. Udrea, Machine recognition of human activities: A survey, Circuits and Systems for Video Technology, IEEE Transactions on 18 (11) (2008) 1473–1488.

[6] L. Wang, D. Suter, Recognizing human activities from silhouettes: Motion subspace and factorial discriminative graphical model, Computer Vision and Pattern Recognition, 2007. CVPR '07. IEEE Conference on (2007) 1–8doi:10.1109/CVPR.2007.383298.

[7] R. Klempous, Biometric motion identification based on motion capture 243 (2009) 335–348.

[8] A. Elgammal, D. Harwood, L. Davis, Non-parametric model for background subtraction (2000) 751–767.

[9] A. Manzanera, J. Richefeu, A new motion detection algorithm based on [sigma]-[delta] background estimation 28 (3) (2007) 320–328.

[10] N. R. Howe, A. Deschamps, Better Foreground Segmentation Through Graph Cuts, ArXiv Computer Science e-printsarXiv:arXiv:cs/0401017.

[11] M. Ahmad, I. Parvin, S.-W. Lee, Silhouette history and energy image information for human movement recognition, Journal of Multimedia 5 (2010) 12–20.

[12] A. Bobick, J. Davis, Real-time recognition of activity using temporal templates, Applications of Computer Vision, 1996. WACV '96., Proceedings 3rd IEEE Workshop on (1996) 39 – 42doi:10.1109/ACV.1996.571995.

[13] R. Mukundan, Moment Functions in image analysis-Theory and applications, World Scientific Publishing Co, 2010.

[14] C. J. C. Burges, A tutorial on support vector machines for pattern recognition, Data Mining and Knowledge Discovery 2 (1998) 121–167.

[15] G. W. Flake, S. Lawrence, Efficient svm regression training with smo (2001).

7. Gesture Recognition of Pathological Gait Markerless

As presented on the "International Joint Conference on Computer Vision, Imaging and Computer Graphics Theory and Applications" VISAPP 2010, february 2010

GESTURE RECOGNITION OF PATHOLOGICAL GAIT MARKERLESS

Fabio Martínez, Juan Carlos León, Eduardo Romero
BioIngenium Research Group, National University of Colombia, Bogotá, Colombia
fmartinezc@unal.edu.co, jcleonal@unal.educo, edromero@unal.educo

Keywords: Gesture Recognition, Human Motion Analysis, Gait Analysis, Markerless Approach

Abstract: Gait patterns may be distorted in a large set of pathologies. In the clinical practice, the gait is studied using a set of measurements which allow identification of pathological disorders, thereby facilitating diagnosis, treatment and follow up. These measurements are obtained from a set of markers, carefully placed in some specific anatomical locations. This conventional procedure is obviously invasive and alters the natural movement gestures, a great drawback for diagnosis and management of the early disease stages, when accuracy is a crucial issue. Instead, markerless approaches attempt to capture the very nature of the movement with practically no intervention on the movement patterns. However, these techniques remain still limited concernig their clinical applications since they do not segment with sufficient precision the human silhouette. This article introduces a novel markerless strategy for classiying normal and pathological gaits, using a temporal-spatial characterization of the subject from 2 differents views. The feature vector is constructed by associating the spatial information obtained with SURF and the temporal information from a Σ-Δ operator. The strategy was evaluated in three groups of patients: normal, musculoskeletal disorders and parkinsons disease, obtaining a sensitivity around 60%

1 INTRODUCTION

Distortion of gait patterns are the first clinical manifestation of many diseases, among others diabetes, brain palsy or accident sequelae. The analysis of human gait attempts to objectively assess pathologies by following up the hidden gait dynamic variables. The set of techniques dedicated to perform this analysis is what is currently known as the gait laboratory, a tool devised to quantify a disease, to compare the gait with normal patterns (Perry and Burnfield, 2010), (Haiyan Luo and et al., 2010). Most of this gait analysis is carried out with a set of markers, carefully placed in some specific anatomical locations. This conventional procedure is invasive and alters the natural movement gestures, necessitating strong variations to achieve diagnosis, i.e., this approach is hardly useful in early stages.

On the other hand, gait dynamic patterns are by nature highly variable and can be easily contaminated with noise. In early stages, most of these diseases differ by very little from what is considered a normal pattern so that classification is a very challenging problem, even for the expert clinicians. This picture may be worsen if one considers that the basic examination tool, the markers, can move very easily or can even be unobservable, contaminating the resulting measurement. These factors together lead to subjective clinical analyses with the consequent limitation in the reproduction of the clinic management of the patient (Kamruzzaman and Begg, 2006), (Wolf and et al, 2006).

Ultimately, this problem has undergone a fundamental transformation since the objective is not anymore the movement reconstruction from the anatomical markers, but the accurate tracking of the movement pattern i.e. the markerless strategy. Research areas as computer vision, automatic surveillance, animation and image processing have already developed some markerless strategies for diverse applications, namely, biometric identification, abnormal motion detection, scene reconstruction and activity classification (Turaga et al., 2008), (Klempous, 2009). How-

ever, there are several problems related to extracting the object of interest from some escenaries, mainly due to the blurred boundaries between the background and foreground (Cristani et al., 2010), (McHugh et al., 2009), an issue that can result in wrong characterizations.

This article presents an efficient markerless methodology to identify and classify different kinds of normal and pathological movements. A non linear Sigma-Delta (Σ-Δ) operator is used to obtain a temporal movement description as a set of pixels. Most of them correspond to a particular patient shape while some small scattered groups belong to the background. Afterwards, we compute a bounding box around of largest group and therein we calculate some local features per frame, using the "Speeded Up Robust Features"(SURF). A weighting function allows associating some of these spatial features with relevant temporal information. This weighted feature vector is used to classify patterns as normal or pathological, applying a classical Support Vector Machine strategy. Evaluation was performed on a database with 96 videos from 32 patients, with three types of movements: normal, musculoskeletal disorders and Parkinson's disease. Sensitivity and specificity are used to assess the utility of this method. This paper is organized as follows: section 2 briefly outlines the nature of the dataset, section 3 introduces the proposed markerless strategy, section 4 sumarizes the results & the effectiveness of the proposed method, finally section 5 concludes with a discussion and possible future works.

2 GAIT DATA

Experimentation was carried out with video sequences recorded from 3 views frontal, lateral and 45 degree view, registered at the gait laboratory of the National University of Colombia, under semi-controlled illumination conditions. This dataset consists of a set of videos captured from 20 patients, each one was recorded 4 times while walking, for a total of 240 video sequences. The Dataset was divided as follows:

- 8 patients diagnosed with musculoskeletal disorders for a total of 13500 frames.
- 7 patients diagnosed with parkinsons disease (No depressive disorder present) for a total of 15500 frames.
- 5 patients with normal gait for a total of 14000 frames

3 THE PROPOSED METHOD

Our proposed method begins calculating the temporal information using a $\Sigma-\Delta$ operator. A bounding box is superimposed upon the region with the largest rate of change and the local features are calculated, within this box, using SURF. A weighting function chooses the more relevant SURF features, those with a similar spatial location to the pixels detected by the $\Sigma-\Delta$ operator, i.e., the features that contain temporal and spatial information. The obtained feature vector is used to classify patterns as normal or pathological, applying a classical SVM, as illustrated in figure 1.

3.1 $\Sigma-\Delta$ Temporal Estimator

Temporal description of the patient gait patterns is central at describing structural changes. Many strategies have been proposed already, they are currently known as background estimation methods (Elgammal et al., 2000), (Manzanera and Richefeu, 2007), (Howe and Deschamps, 2004). These methods use a sequence of images I_t and build up a model of the static scene M_t. The model output is an image D_t, where the background is represented by $D_t(x) = 0$ and the foreground is $D_t(x) = 1$.

Algorithm 1 $\Sigma-\Delta$ Algorithm

```
Initialization: M_0(x) = I_0(x)
for each Frame t do
    M_t(x) = M_{t-1}(x) + sgn(I_t x − M_{t-1}(x))
    Δ_t(x) = |M_t(x) − I_t x|
end for
Initialize: V_0(x) = Δ_t(x)
for each Frame t do
    for each pixel x such that Δ_t(x) ≠ 0 do
        V_t(x) = V_{t-1}(x) + sgn(N × Δ_t(x) − V_{t-1}(x))
        if Δ_t(x) < V_t(x) then
            D_t(x) = 0
        else
            D_t(x) = 1
        end if
    end for
end for
```

In our dataset the silhouette extraction is a difficult task because of the similarity between the foreground and the background. Hence we use a non linear $\Sigma-\Delta$ operator to obtain a motion descriptor which detects the most probable localization of the foreground. This estimator oversamples a signal at higher rates than the especified by the Nyquist teorem, increasing correlation between the adjacent frames at each pixel (Manzanera and Richefeu, 2007). The $\Sigma-\Delta$ operator behaves as a background tracker $M_t(x)$, dynamically updated by comparing each image $I_t(x)$ with the current

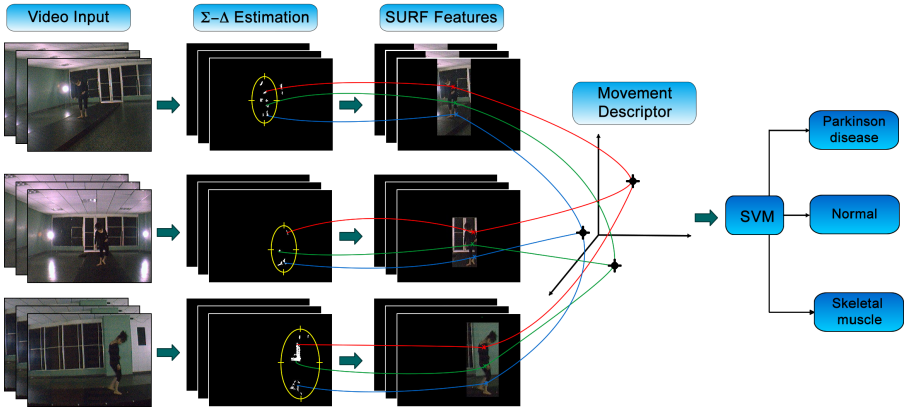

Figure 1: Markerless strategy consists in determining a feature vector to describe normal and pathological movement, using a temporal-spatial gait characterization. Motion is classified using a Support Vector Machine strategy

background $M_t(x)$, using a simple updating rule: If $I_t(x)$ is greater (lower) than $M_t(x)$, then a positive increase (decrease) $+\Delta$ is performed. The implemented $\Sigma-\Delta$ is shown in the Algorithm 1.

Upon the region with the largest movement pattern, we compute a center of mass, on top of which we place a bounding box that contains the object of interest. This process is speeded up using an integral image representation of the original images, reducing the computational cost by 94% (Viola and Jones., 2004).

3.2 Speeded Up Robust Features (SURF)

Once the bounding box is extracted, we calculate some local features of it using the Speeded Up Robust Features (SURF) descriptor (Herbert Bay and Gool, 2008). This descriptor highlights the salient points within the bounding box so that each salient point is described by magnitude, orientation and feature vectors. The SURF method provides invariant image description, allowing a robust representation against illumination, scale and rotation changes, a useful aspect in our problem due to the semi-controlled scenario, different views and patients.

The SURF description is obtained by initially computing the Hessian matrix $H(X,\sigma)$, as follows: -

$$H(X,\sigma) = \begin{bmatrix} L_{xx}(X,\sigma) & L_{xy}(X,\sigma) \\ L_{xy}(X,\sigma) & L_{yy}(X,\sigma) \end{bmatrix}$$

where X is a especific point, σ is the scale and $L_{xx}(X,\sigma)$ is the second Gaussian convolution. This step relies on an integral image to reduce the computational time. Afterwards, SURF constructs a circular region surrounding the points of interest, attempting to assign a unique orientation by estimating the Haar wavelet coefficients in both directions and thereby gaining invariance to image rotations. SURF descriptors are thus constructed by extracting square regions around the points of interest, which are divided in four sub-regions.

3.3 Feature Extraction

SURF features are used to obtain a summarization of the gait sequence, they operate exclusively on the bounding boxes. Once the set of SURF features is calculated, the values of the SURF descriptor vector are weighted, following the pixel intensity distribution obtained from the $\Sigma-\Delta$ operator. Higher values are assigned to vectors whose locations belong to regions with high movement. The proposed summarization is a collection of weighted vectors, arranged acording to their frame number, on the gait sequence.

As the SURF features produce a variable number of points of interest for different squences, the final descriptor of a gait sequence is obtained at quantizing the complete set of vectors into 5,10,20,40 and 50 clusters using the Expectation Maximization algorithm yielding 5 different descriptors for a single sequence.

4 Experimental Results

Classifcation was performed using a Support Vector Machine (SVM) trained with a set of attribute vectors, extracted from labeled gait sequences. In this phase, two types of kernels were used, polynomial and Radial Basis Function (RBF) kernels. Parameters of the cost function, gamma (RBF kernels) and the exponent (polynomial kernels) were estimated using the sequential minimal optimization algorithm (Flake and Lawrence, 2001).

Class	Presicion	Recall	Sensitivity
Musculo-eskeletical	0.75	0.75	0.75
Normal	0.7	0.66	0.65
Parkinson	0.61	0.64	0.65
Total	0.68	0.68	0.68

Table 1: Presicion, Recall and Sensitivity using Polinomial Kernel

Class	Presicion	Recall	Sensitivity
Musculo-eskeletical	0.67	0.33	0.33
Normal	0.6	0.95	0.95
Parkinson	0.72	0.41	0.47
Total	0.66	0.64	0.64

Table 2: Presicion, Recall and Sensitivity using RBF Kernel

Tables 1 and 2 summarize the precision, recall, and sensitivity reproted by our method and the tables 3 and 4 report a confusion matrices for the best 3 classifiers found. Overall The proposed methodology can classify pathological and normal gait patterns with a sensivity and precision above 60% in semi-controlled environments. The proposed classifiers seem to favor descriptors built upon lower number of clusters, as two of the best 3 classifiers use the data with 5 clusters and the other works with 20 clusters.

5 Conclusion

This paper has introduced a novel markerless method that allows to characterize normal and pathological human gait patterns. The whole markerless strategy consists in determining a feature vector for describing normal and pathological movement, using a temporal-spatial gait characterization from 3 differents views. The feature vector is constructed by associating the spatial information obtained from SURF and the temporal information from a $\Sigma - \Delta$ operator. Motion is classified using a classical Support Vector Machine strategy. Results demonstrate that this method can complement the conventional gait analysis since it assigns objective pattern measurements. The methodology presented in this work constitutes a first approximation to understanding the complex dynamic of the gait. From this kind of analyzes, we expect it would be possible to set up an assembly of descriptors which allow to accurately describe motions patterns and quantify gait semantics.

Class	Musculo-eskeletical	Normal	Parkinson
Musculo-eskeletical	9	1	2
Normal	2	14	5
Parkinson	1	5	11

Table 3: Confusion Matrix using Polynomial Kernel

Class	Musculo-eskeletical	Normal	Parkinson
Musculo-eskeletical	4	5	3
Normal	1	20	0
Parkinson	1	8	8

Table 4: Confusion Matrix using RBF Kernel

REFERENCES

Cristani, M., Farenzena, M., Bloisi, D., and Murino, V. (2010). Background subtraction for automated multisensor surveillance: A comprehensive review. *EURASIP Journal on Advances in Signal Processing*, 24:17.

Elgammal, A., Harwood, D., and Davis, L. (2000). Nonparametric model for background subtraction. pages 751–767.

Flake, G. W. and Lawrence, S. (2001). Efficient svm regression training with smo.

Haiyan Luo, S. C. and et al., D. W. (2010). A remote markerless human gait tracking for e-healthcare based on content-aware wireless multimedia communications. *IEEE Wireless Communications,*.

Herbert Bay, Andreas Ess, T. T. and Gool, L. V. (2008). Speeded-up robust features (surf). *Comput. Vis. Image Underst*, 110:346359.

Howe, N. R. and Deschamps, A. (2004). Better Foreground Segmentation Through Graph Cuts. *ArXiv Computer Science e-prints*.

Kamruzzaman, J. and Begg, R. K. (2006). Support vector machines and other pattern recognition approaches to the diagnosis of cerebral palsy. *IEEETrans. Biomed. Eng.*, 53:2479–2490.

Klempous, R. (2009). Biometric motion identification based on motion capture. 243:335–348.

Manzanera, A. and Richefeu, J. (2007). A new motion detection algorithm based on [sigma]-[delta] background estimation. 28(3):320–328.

McHugh, J., Konrad, J., Saligrama, V., and Jodoin, P.-M. (2009). Foreground-adaptive background subtraction. *Signal Processing Letters, IEEE*, 16(5):390 –393.

Perry, J. and Burnfield, J. M. (2010). *Gait Analysis: Normal and Pathological Function*. NJ.Slack.

Turaga, P., Chellappa, R., Subrahmanian, V. S., and Udrea, O. (2008). Machine recognition of human activities: A survey. *Circuits and Systems for Video Technology, IEEE Transactions on*, 18(11):1473–1488.

Viola, P. and Jones., M. J. (2004). Robust real-time face detection. *Int. J. Comput. Vision,*, 57:137 154.

Wolf, S. and et al, T. L. (2006). Automated feature assessment in instrumented gait analysis. *Gait and Posture*, 23:331–338.

8. Model Based Analysis of Gait Patterns

This chapter presents a markeless strategy to characterize gait patterns in a video sequence. Unlike the previous, this approach closely follows the steps presented in section 2.1.1 for the markerless analysis of human gait, here a structural model of the lower limbs is used as the main source of information.

Our main goal is to establish the alignment of the lower limbs during a gait sequence, this will allow us to compare the dynamics of normal and pathological patients.

Overall we approach this task, as a filtering problem, where the hidden states are the alignments of the lower limbs during a gait cycle and the observations are the estimation of the human silhouette.

The first step is to select a sub-set of frames which contains a full gait cycle of the right leg for every patient. There are two main motivations for this choice: First, all the video captures were made from a sagital point of view, under this set-up one of the legs is occluded during some intervals of the gait cycle, in our sequences the right leg occludes the left. Second: Parkinson's Disease is a degenerative disorder of the central nervous system, thus altered gait patterns must be observed in both lower limbs.

For the estimation of the human silhouette each subset of frames is processed with the extension of the Σ - Δ Estimation[1] presented in chapter 5. Then we use a model to generate a set of possible alignments of the lower limbs (hidden states of the filtering problem). Every generated template is then transformed into squares, so that a template can be matched to the output of the background subtraction as proposed by Mohr et al.[40] (see section 8.3).

The processed gait sequences, the transformed template set and the matching strategy are used in a particle filter strategy. The result of this process for each frame is the most likely configuration of the lower limbs. Each estimated configuration is stored and then whole set of angles estimated at the lower limbs is used for characterization of the gait as presented on section 8.4.

[1] We exclude the final step that classifies the pixels as background or foreground, as this process would yield a binary image which can not be properly matched with the model's templates.

8.1. Human Gait Models

A gait model is an a priori knowledge of the observed gait pattern, such models are commonly used to define a set of valid configurations of the body parts that are considered relevant for an analysis and the possible transitions between configurations. According to the strategy used to define the set of configurations and transitions, we can distinguish two types of models[1, 11]:

Structural Models Whose configurations provide knowledge on the approximate geometric structure of the body parts in motion. But provide little information on the transitions between states.

Bio-Mechanical Models Which explicitly model the participation of muscles, bones, tendons and other tissues considered relevant in human gait. In these models the geometric structure and possible transitions are a result of the modeled interactions of the participating elements.

In this work, we use a structural model of the lower limbs, whose valid poses are defined by the average angles created during a gait cycle of a normal person. As the data used to generate these configurations is ordered from the beginning to the end of a gait cycle, the model also provides information on the possible state transitions.
The model generates the angles between: torso and thigh (Hip Flexion Extension), tight and shin (Knee Flexion Extension), shin and foot (Plantar Flexion). While these are not all the possible angular displacements of the lower limbs during a gait cycle, these are the most relevant to analyze a walking sequence captured from a sagital view.
These angles allow to locate and rotate truncated cones to simulate the movement of the lower limbs, our model has 3 cones for each limb, which represent the tight, shin and foot, an additional cone represents the waist see figure **8-1**. With this setup we are capable of producing 100 different templates that are used as prior for the tracking step.

8.2. Filtering

A filtering problem consists of a recursive estimation of the state of a dynamic system from a set of observations [17], formally the system changes states according to:

$$X_t = f(X_{t-1}, W_t) \tag{8-1}$$

Where X_t is the state of the system at time t, W_t is a noise present on the transition process at time t and f is a state transition function. The set of states X_t can not be directly observed, instead an observable state Z_t is generated by:

$$Z_t = h(X_t, V_t) \tag{8-2}$$

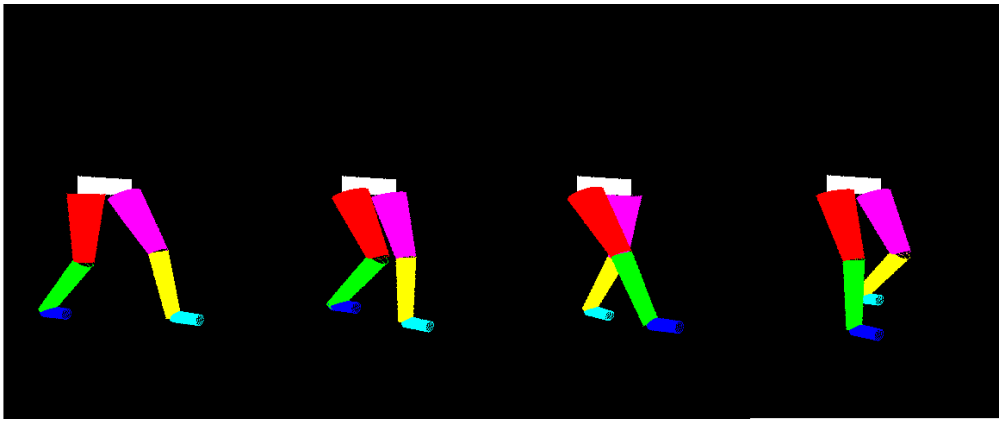

Figure 8-1.: Sample model poses during a gait cycle

Where h maps from the space state X_i into the observations space Z_i and V_t is noise on the observations at time t. The main goal of a filtering strategy is to build an estimate of the hidden set of states X_i by analyzing a temporal sequence of observable and noisy Z_i states. There are optimal solutions to filtering problems, nevertheless these solutions apply for specific conditions. One of the best known is the kalman filter[34], which assumes that f is linear and noises W and V are Gaussian and uncorrelated, this assumptions allow to derive a solution to the filtering problem in terms of means and covariances. A more general solution requires a different approach.

8.2.1. Bayesian Filtering

A Bayesian approach to a filtering problem, does not relies on characteristics of function f (or its parameters) neither makes direct assumptions over noises W and V, but rather attempts to estimate a posterior probability $p(X_t|Z_{1:t})$ based on available information[34]. While a general analytic expression for $p(X_t|Z_{1:t})$ can not be obtained[7], a recurrence expression can be built if the likelihood $p(Z_t|X_t)$ and posterior pdf at time $t-1$ are known (or can be approximated)[34]. Under this conditions the posterior can be written by means of the Chapman Kolmogorov equation as[2]:

$$p(X_t|Z_{1:t-1}) = \int p(X_t|X_{t-1})p(X_{t-1}|Z_{1:t-1})dX_{t-1} \tag{8-3}$$

Later at time t, when Z_t is observable, the prior might be updated using the bayes rule:

$$p(X_t|Z_{1:t}) = \frac{p(Z_t|X_t)p(X_t|Z_{1:t-1})}{p(Z_t|Z_{1:t-1})} \tag{8-4}$$

[2]The derivation of this equations can be found in appendix A

Where the normalization term is also a recurrence

$$p(Z_t|Z_{1:t-1}) = \int p(Z_t|X_t)p(X_t|Z_{1:t-1})dx_t \tag{8-5}$$

Notice that equations 8-4 and 8-5 depend on the likelihood function $p(Z_k|X_k)$, which is an approximation of the map $Z_k = h(X_k, V_k)$, also equation 8-3 implies some knowledge on the transition function f to build $p(X_t|X_{t-1})$. The solution to the filtering problem using a Bayesian framework can only be approximated if there exists some knowledge of (prior on) the dynamic system.
Again the recursions above can not be solved analytically[4], however they can be approximated algorithmically. Amongst the best known approximations are Monte Carlo methods, where the posterior probability is estimated by a set of weighted random samples as follows: Let $p(X|Z_t)$ represent the knowledge of model state X obtained from observations Z up to time t, it can be represented by a set of N particles $\{p_t^1, p_t^2, ..., p_t^N\}$ and a set of associated weights $\{w_t^1, w_t^2, ..., w_t^N\}$, where the weight assignation $w_t^i \propto p(Z_t|X = p_t^i)$, hence posterior for state X_k can be approximated by its expected value[16].

$$p(X|Z_t) \approx E[X] = \sum_{i=1}^{N} w_t^i p_t^i \tag{8-6}$$

As the number of samples grows, the estimate $E[X]$ is closer to the actual pdf. With a very large set of samples this characterization becomes an equivalent representation to the posterior pdf.[17].

8.2.2. The Annealed Particle Filtering

The Annealed Particle Filtering (APF) is one of the Monte Carlos methods used to estimate the posterior pdf. It is based on the simulated annealing method, which approaches the minimum of a function $u(x)$ by drawing samples from a distribution created over the target function, it is defined as[16]:

$$p(x) = Ce^{-\lambda u(x)} \tag{8-7}$$

With C a normalization constant.
Notice that a small λ generates a broad distribution with peaks around the smallest values of u, as λ grows the probability mass concentrates on the minimum of u. This behavior can be used to find the minimum of function u in an iterative process, which starts by randomly drawing samples $\{s_i^0\}$ from p with an initial small λ_0, then λ_0 is increased to λ_1 and a new set of samples $\{s_j^1\}$ is drawn, this time, samples are generated from both the distribution $p(x)$ and the last drawn samples $\{s_i^0\}$, λ_i keeps growing and new set of samples are drawn again, on the long run, the samples drawn $\{s_i^n\}$ with a large λ_n approach the minimum of the function.

The same strategy is used on the APF to approach the posterior $p(X|Z)$ at time t by a series of posteriors $p^i(X|Z)$ with $0 \leq i \leq n$, the transitions between the posteriors on this sequence are determined by the values of the weighting function.
Overall the steps for an APF can be written as:[15]:

1. At time t an annealing run is started at layer M, let $m = M$

2. Each layer of the current annealing run is initialized with unweighted particles $P_{k,m}$.

3. Each of these particles is then assigned a weight

   $w^i_{k,m} \propto w(Z_k, p^i_{k,m})$

   These weights are normalized so that: $\sum w^i_{k,m} = 1$, the resulting set of weighted particles is noted as $P^w_{k,m}$

4. N particles are draw randomly form $P^w_{k,m}$, with probability equal to their weight, these particles are used to generate the next particle layer by:

   $p^n_{k,m-1} = p^n_{k,m} + B$

   Where B is multivariate Gaussian noise with mean 0.

5. The process is repeated from step 1 until layer 0 is reached

6. The final set $P^w_{k,0}$ is used to estimate the most likely state configurations as

   $$X_k = \sum_{i=0}^{N} w^i_{k,0} p^i_{k,0}$$

The outlined algorithm does not have an explicit initialization process that provides an initial state estimation (set of particles) at time $t = 0$. We solve this issue by an special annealing run on the first frame on which a particle is assigned to every possible model configuration on every possible position of the frame, the results of this runs are the set of particles at time $t = 1$, where the annealing continues as presented above.
This special first run obviously generates a very large set of particles which increases the running time of the algorithm, however the weighting process of each particle works independently, and parallelization can be easily achieved to compensate for the extra amount of particles. Our implementation uses a 6 core CPU (12 logical cores) and is able to process gait cycles of approximate 40 frames in an average of 12 minutes, where the initial annealing run takes about $\frac{1}{4}$ of the total processing time.

8.3. Matching

As stated in section 8.2.1 a critical step on the estimation of the posterior on Bayesian Filtering is the estimation of the likelihood $p(X|Z)$ (or weighting function for the APF). As our prior is a structural model from which a series of images can be obtained representing each of its configurations, a template matching strategy is a natural choice for the estimation of $p(X|Z)$.
A template Matching problem with an image I and a template M can be stated as finding a transformation T of the pixel coordinates of M, such that it brings M to a location on I that gives a best match for a given distance measure d [19]:

$$\max_T d(T(M), I) \tag{8-8}$$

Several distance measures can be built between the template image and the image sequence, however there is a restriction on the chosen function: it must be evaluated over a very large set of particles during several annealing runs in many frames, hence we need a function that can be efficiently evaluated.
As we have a single object of interest on the image (the right leg) and a template whose shape must match that object, we choose a very simple and well known distance measure where a template has a best match if it completely overlaps the object of interest and no part of the template overlaps a region outside of the object of interest.

8.3.1. Matching Algorithm

To find the pose of the right leg at a given frame we use a known template matching strategy for articulated objects proposed by Mohr et al. [40]. Where each template is represented by a set of mutually disjoint rectangles R_s, allowing to represent the probability of finding a template at position p by means of the covered and uncovered areas of R_s when shifted to position p. This computation is speedup by means of an integral image[55] I, formally:

$$P_s(p) = \sum_{R_i \in R_s} (I((v_x^i, v_y^i) + p) + I((u_x^i, u_y^i) + p) - I((v_x^i, u_y^i) + p) - I((u_x^i, v_y^i) + p))) \tag{8-9}$$

Where u^i and v^i are the upper left corner and lower right corner of the rectangle R_i.

Mohr et al. also consider the background distribution $P_{\bar{s}}(p)$ which has the same formula as equation 8-9 but the rectangle set R_s covers the background instead of the the template. This yields a final form for the probability of finding a template at position P as:

$$P(p) = e^{\frac{1}{2}(P_s^n(p) + P_{\bar{s}}^n(p))} \tag{8-10}$$

Where $P_s^n(p)$ and $P_{\bar{s}}^n(p)$ are resolution independent (normalized) forms of 8-9 for the foreground and background respectively. However, as we do not deal with different resolutions

of the templates or the images on the video, but rather with different template shapes (to adapt to the anatomical variability of our patients), we limit ourself to the unnormalized forms of P_s and $P_{\bar{s}}$ for equation 8-10 and normalize over the results for a given frame.
Another difference of our matching scheme is that we do not build a template hierarchy to increase the overall performance of the matching process, as for the particle filter we need a probability estimation for every template.

8.4. Pathological Gait Characterization

Our dataset is composed of 12 patients, 6 normal subjects and 6 patients with parkinson's disease, whose gait sequences were captured from a sagital view at the gait laboratory of the Universidad Nacional de Colombia, under semi-controlled illumination conditions.
For the characterization of the gait patterns we initially apply the procedure described earlier in this chapter, and compare the estimated angles during a gait cycle of a given patient with the average patterns of a normal person. We use the Frechet distance to quantify their similarity.
The Frechet distance (δ_F) is a measure of similarity between curves that takes into account the location and ordering of the points along the curves[18]. Informally the Frechet distance can be thought as the length of the shortest leash that joins a dog and its owner, when one of them walks on curve f and the other on curve g under the condition that any of them can change its speed, butbacktracking is not allowed.

Formally: let f and g be curves defined by $f : [a, b] \to V$ and $g : [a', b'] \to V$ the Frechet distance between these curves is defined as:

$$\delta_F(f, g) = \inf_{\alpha,\beta} \max_{t\in[0,1]} d(f(\alpha(t)), g(\beta(t))) \tag{8-11}$$

Where α and β are arbitrary continuous nondecreasing functions[3] from $[0, 1]$ to $[a, b]$ and $[a', b']$ respectively.

Figures **8-2** and **8-3** show how the Frechet distance is used in our analysis: the first shows the estimated values of the hip flexion extension (HFE) angle of a normal subject of our dataset (red curve) along with the average angles for a normal person (blue curve) during a gait cycle, the second one shows this same average along with the estimated the hip flexion extension angles of a patient with Parkinson's Disease of our dataset. Notice how the estimated angles for the healthy subject closely resembled those of the average normal pattern which yields a small Frechet distance. For the Parkinson patient the overall shape of the estimated angles resembles those of the normal pattern, however it has a smaller amplitude which yields a larger Frechet distance.

[3]Non decreasing functions assure that backtracking is not allowed

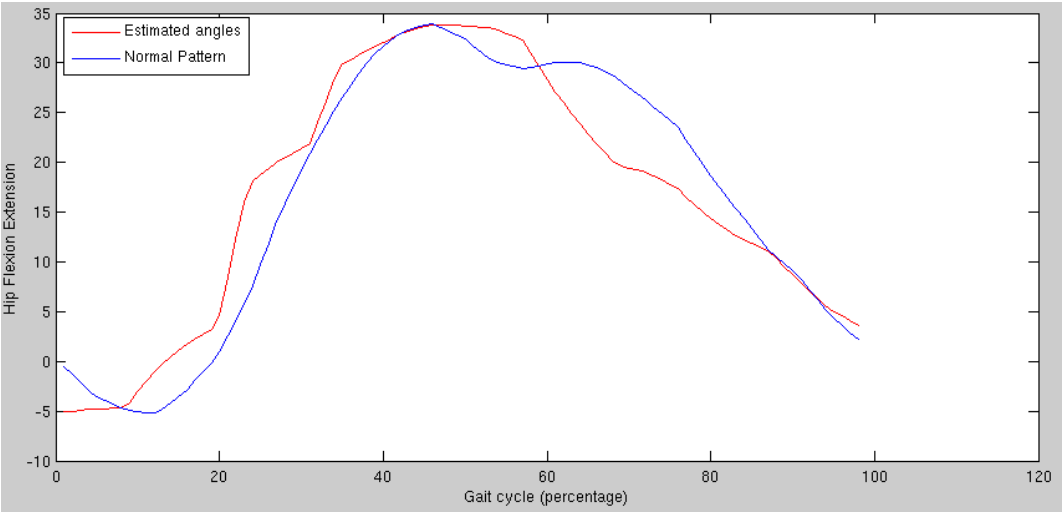

Figure 8-2.: Hip Flexion Extension comparison, normal average pattern (blue) and the pattern of a normal subject (red)

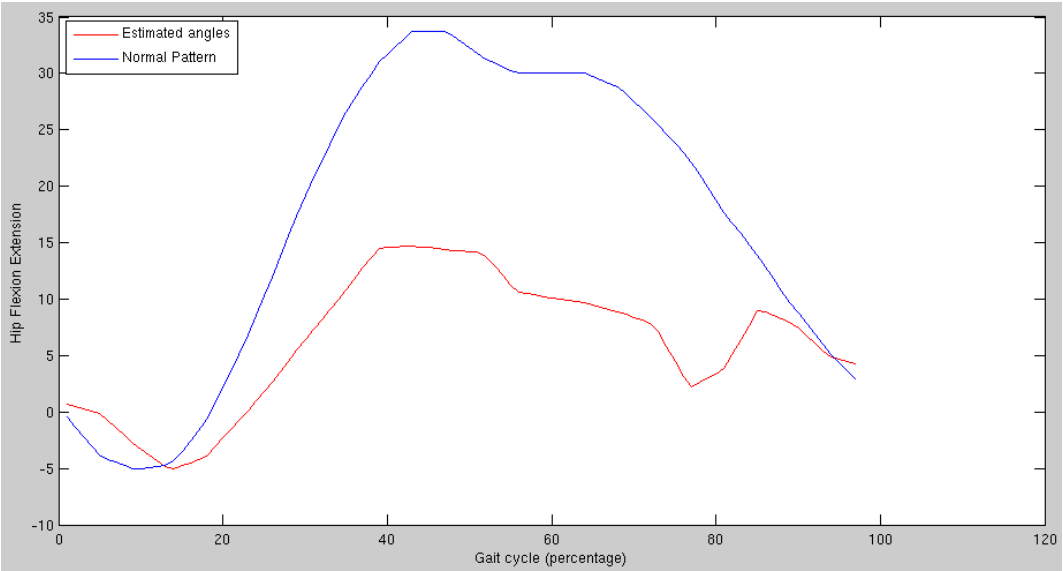

Figure 8-3.: Hip Flexion Extension comparison, normal average pattern (blue) and the pattern of patient with parkinson (red)

8.4.1. Results

The calculated Frechet distances for each patient are summarized in table **8-1**, per group averages are shown in table **8-2**

The angle created between the shin and foot is not used for this characterization as the segmentation step yields poor results for the feet, this is due to the capture conditions where

Patient	Group	δ_F Hip Flexion Extension	δ_F Knee Flexion Extension
am	Normal	22.80	40.39
ar	Normal	37.91	53.02
ca	Normal	55.39	53.03
hl	Normal	24.42	38.63
jc	Normal	27.55	42.49
mg	Normal	33.31	41.56
es	Parkinson	62.84	51.68
fm	Parkinson	38.25	65.8
hg	Parkinson	55.09	63.97
jj	Parkinson	66.46	69.36
mv	Parkinson	95.63	111.51
ni	Parkinson	77.27	33.8

Table 8-1.: Frechet distances calculated for the angles hip flexion extension & knee flexion extension for all patients

Group	δ_F HFE	δ_F KFE
Normal	33.56 $\pm$ 12.09	44.85 $\pm$ 6.45
Parkinson	64.92 $\pm$ 18.96	66.02 $\pm$ 25.8

Table 8-2.: Means and standard deviations for the groups of normal and Parkinson patients

the patients are dressed in a black suit and the platform where they walk is also black.

Results show that, in average, normal patients have a smaller Frechet distance to the average normal pattern for both measured angles. The angles measured for the knee flexion extension (KFE) seem to be particularly useful for characterization as the mean of both classes largely differs and standard deviations are small compared to this distance.

Results also show that normal patients have a smaller inter class variability for both measured angles, especially for the knee flexion extension, this means that under the proposed approach is much easier to characterize normal gait patterns than characterize parkinsonian gait patterns.

8.5. Conclusions

The proposed strategy for markeless characterization of gait patterns using the Σ - Δ estimation for background subtraction, an structural model for state generation, and particle filter for belief estimation is effective, as it allows to estimate the dynamics of the lower limbs

from on a video sequence of both normal and parkinsonian gait.

The frechet distance is an effective metric to characterize the normal and parkinsonian gait patterns, by comparing them to an average pattern, especially when applied to the estimations of the KFE angles.

9. Conclusions and Future Work

This thesis has explored the problem of the characterization of gait patterns with markerless strategies in the Parkinson Disease, both model-less and model-based approaches were presented.

The main motivation for a markerless analysis of the Parkinson's Disease was the well known drawbacks of marker-based analysis (as inaccurate placement, and displacement of the underlying skin), the altered gait patterns on the Parkinson's Disease, and the fact that a bio-marker directly related to the degenerative process characteristic of Parkinson's Disease remains unknown.

One of the fundamental tools in markerless analysis of human motion is the background segmentation, as it allows to detect and follow moving objects along videos sequences. This segmentation process was part of the work on this thesis and the results are in chapter 5, where an extension of the Σ - Δ estimation for background subtraction is introduced. This extension enhances the pixel description with local features, allowing a multiscale representation of each frame, this improves the detection of the lower limbs, a key task for the markerless analysis of gait.

The first strategies presented for markerless analysis are model-less strategies based on segmentation of the human silhouette and the extraction of visual descriptors from it. Chapter 6 approaches the analysis of human gait by the construction of a motion history images with the silhouettes extracted from a gait sequence, these images summarize the movements on a gait sequences and are used for gait classification in a classical SVM approach. Chapter 7 presented an strategy which associated the spatial information obtained from SURF features with the the temporal information obtained from the Σ - Δ operator, again a summarization was built and a classic SVM approach was used for classifications.

Chapter 8 presented a more complex, model based, approach for the characterization of human gait, centered on the recognition of the pose of the lower limbs during a gait sequence, a problem which is approached with a Bayesian filtering strategy that uses an structural model of the human leg as prior. The Frechet distance is used to obtain measure of the difference between gait patterns.

There remain at least two interesting topics to continue with the work presented in this thesis. The first is to further explore the features on the images and the summarizations presented on chapters 6 and 7 in order to understand which characteristics are the most discriminative, such and understanding might not only improve the performance of the classification but might also allow to simplify the analysis of the descriptor and even the construction of new ones. The second is to use a more complete model of the human body in the approach proposed on chapter 8, such a model would enable a more complete analysis of the parkinsonian gait, where some features as larger double stance and lean forward stance could be properly measured.

Ultimately, these works might lead to a better quantification and representation of patters on the parkinsonian gait, which would allow the assessment of the disease but most importantly will be helpful to objectively estimate its progression.

A. Derivation of relevant Particle Filter Equations

The Chapman-Kolmogorov equation is an identity for transition densities on a Markovian stochastic process, defined as:

$$p(X_n|X_s) = \int p(X_n|X_r)f(X_r|X_s)dX_r \tag{A-1}$$

Let Z_i be the set of noisy observations, and X_i the set of unobservable states on a filtering problem as presented in chapter 8. A recurrence expression for $p(X|Z)$ can be found using equation A-1 if the posterior at time $t-1$ $p(X_{t-1}|Z_{t-1})$ and the dynamics of the system $p(X_t|X_{t-1})$ are know or can be approximated[4].

$$p(X_t|Z_{1:t-1}) = \int p(X_t|X_{t-1})p(X_{t-1}|Z_{1:t-1})dX_t \tag{A-2}$$

Notice that $p(X_t|Z_{t-1})$ is a prior on the state distribution at time t, also at time t Z_k becomes observable which allows to estimate a likelihood $p(Z_t|X_t)$. With a prior and a likelihood Bayes rule can be applied to obtain a posterior[4]:

$$p(X_t|Z_t) = \frac{p(Z_t|X_t)p(X_t|Z_{1:t-1})}{p(Z_{1:t})} \tag{A-3}$$

Using the same argument as above, the denominator can also be expressed as a recurrence:

$$p(Z_{1:t}) = P(Z_t|Z_{1:t-1}) = \int p(Z_t|X_t)p(X_t|Z_{1:t-1})dx_t \tag{A-4}$$

$p(X_t|Z_t)$ is the posterior probability that must be estimated in a Bayesian approach to a filtering problem.

Bibliography

[1] Aggarwal, J. K. ; Cai, Q.: Human Motion Analysis: A Review. En: *Computer Vision and Image Understanding* 73 (1999), p. 428–440

[2] Andlin-Sobocki, Patrik ; Joensson, Bengt ; Wittchen, Hans-Ulrich ; Olesen, Jes: Costs of Disorders of the Brain in Europe. En: *EUROPEAN JOURNAL OF NEUROLOGY* 12 (2005)

[3] Andriacchi, Thomas P. ; Alexander, Eugene J.: Studies of human locomotion: past, present and future. En: *Journal of Biomechanics* 33 (2000), Nr. 10, p. 1217 – 1224. – ISSN 0021–9290

[4] Arulampalam, Sanjeev ; Maskell, Simon ; Gordon, Neil ; Clapp, Tim: A Tutorial on Particle Filters for On-line Non-linear/Non-Gaussian Bayesian Tracking. En: *IEEE Transactions on Signal Processing* 50 (2001), p. 174–188

[5] Baker, Richard: Gait analysis methods in rehabilitation. En: *Journal of Neuroengineering and Rehabilitation* 3 (2006)

[6] Benezeth, Y. ; Jodoin, P.M. ; Emile, B. ; Laurent, H. ; Rosenberger, C.: Review and evaluation of commonly-implemented background subtraction algorithms. (2008), dec., p. 1 –4. – ISSN 1051–4651

[7] Bergman, Niclas: *Recursive Bayesian Estimation Navigation and Tracking Applications*, LinkÂ¨oping University, Tesis de Grado, 1999

[8] Bond, Jaqueline M.: Goal-directed secondary motor tasks: Their effects on gait in subjects with parkinson disease. En: *Archives of Physical Medicine and Rehabilitation* 81 (2000), Nr. 1, p. 110 – 116. – ISSN 0003–9993

[9] Bourdopoulos, George I. ; Pnevmatikakis, Aristodemos ; Anastassopoulos, Vassilis ; Deliyannis, Theodore L.: *Delta-Sigma Modulators Modeling, Design and Applications*. Imperial College Press, 2003

[10] Christine, Chadwick W. ; MD, Michael J. A.: Clinical differentiation of parkinsonian syndromes: Prognostic and therapeutic relevance. En: *The American Journal of Medicine* 117 (2004), Nr. 6, p. 412 – 419. – ISSN 0002–9343

[11] Cifuentes, Christian ; Martinez, Fabio ; Romero., Eduardo: Analisis Teorico y Computacional de la Marcha Normal y Patologica: una Revision. En: *Revista Med* 18 (2010), p. 182–196

[12] Colcher, Amy ; Simuni, Tanya: CLINICAL MANIFESTATIONS OF PARKINSON'S DISEASE. En: *Medical Clinics of North America* 83 (1999), Nr. 2, p. 327 – 347. – ISSN 0025–7125

[13] Das, Resul: A comparison of multiple classification methods for diagnosis of Parkinson disease. En: *Expert Systems with Applications* 37 (2010), Nr. 2, p. 1568 – 1572. – ISSN 0957–4174

[14] Davis, Roy B. ; Ounpuu, Sylvia ; Tyburski, Dennis ; Gage, James R.: A gait analysis data collection and reduction technique. En: *Human Movement Science* 10 (1991), Nr. 5, p. 575 – 587. – ISSN 0167–9457

[15] Deutscher, Jonathan: Articulated body motion capture by annealed particle filtering, 2000, p. 126–133

[16] Deutscher, Jonathan ; Reid, Ian: Articulated Body Motion Capture by Stochastic Search. En: *International Journal of Computer Vision* 61 (2005), p. 185–205. – 10.1023/B:VISI.0000043757.18370.9c. – ISSN 0920–5691

[17] Doucet, Arnaud ; Godsill, Simon ; Andrieu, Christophe: On Sequential Monte Carlo Sampling Methods for Bayesian Filtering. En: *STATISTICS AND COMPUTING* 10 (2000), Nr. 3, p. 197–208

[18] Eiter, Thomas ; Mannila, Heikki: Computing discrete Frechet distance / Technische Universitaet Wien. 1994. – Informe de Investigación

[19] Fredriksson, Kimmo: *Rotation Invariant Template Matching*, University of Helsinki, Tesis de Grado, 2001

[20] Grace, Peter M.: *Two methods of biomarker discovery: applications in neuropathic pain and pharmacotherapy*, The University of Adelaide, Tesis de Grado, 2010

[21] Group, NHI Biomarkers Definitions W.: Biomarkers and surrogate endpoints: preferred definitions and conceptual framework. En: *Clinical Pharmacology and Therapeutics* (2001), p. 89–95

[22] Henao, Lorenza: *Extraccion y Seguimiento de los Miembros Inferiores Durante la Marcha*, Universidad Nacional de Colombia, Tesis de Grado, 2011

[23] Henchcliffe, Claire ; Dodel, Richard ; Beal, M. F.: Biomarkers of Parkinson's disease and Dementia with Lewy bodies. En: *Progress in Neurobiology* (2011), Nr. 0, p. –. – ISSN 0301–0082

[24] Jankovic: Parkinson's disease: clinical features and diagnosis. En: *Journal of Neurology Neurosurgery Psychiatry* (2008), p. 368–376

[25] Karen M Ostrosky, Ray G B. ; Gee, Zena: A Comparison of Gait Characteristics in Young and Old Subjects. En: *Journal of the American Physical Therapy Association* 74 (1994), p. 637–644

[26] Korczyn, AD: Cognitive dysfunction in Parkinson's disease. En: *Annals of General Hospital Psychiatry* 2 (2003)

[27] Lang, Anthony E. ; Lozano, Andres M.: Parkinson's Disease. En: *New England Journal of Medicine* 339 (1998), Nr. 15, p. 1044–1053

[28] de Lau, Lonneke M. ; Breteler, Monique M.: Epidemiology of Parkinson's disease. En: *The Lancet Neurology* Volume 5 Issue 6 (2006), p. 525–535

[29] Leardini, Alberto ; Chiari, Lorenzo ; Croce, Ugo D. ; Cappozzo, Aurelio: Human movement analysis using stereophotogrammetry: Part 3. Soft tissue artifact assessment and compensation. En: *Gait & Posture* 21 (2005), Nr. 2, p. 212 – 225. – ISSN 0966–6362

[30] Lees, Andrew J. ; Hardy, John ; Revesz, Tamas: Parkinson's disease. En: *The Lancet* 373 (2009), Nr. 9680, p. 2055 – 2066. – ISSN 0140–6736

[31] Lord, S E. ; Halligan, P W. ; Wade, D T.: Visual gait analysis: the development of a clinical assessment and scale. En: *Clinical Rehabilitation* 12 (1998), Nr. 2, p. 107–119

[32] Lu, TW ; O'Connor, JJ: Bone position estimation from skin marker co-ordinates using global optimisation with joint constraints. En: *Journal of Biomechanics* 32 (1999), p. 129–134

[33] Manzanera, Antoine ; Richefeu, Julien C.: A new motion detection algorithm based on Sigma Delta background estimation. En: *Pattern Recognition Letters* 28 (2007), Nr. 3, p. 320 – 328. – ISSN 0167–8655

[34] Maskell, S. ; Gordon, N.: A tutorial on particle filters for on-line nonlinear/non-Gaussian Bayesian tracking. Workshop (2001), oct., p. 2/1 – 2/15 vol.2

[35] Meg E Moris, Robert Iansek Jeffrey S.: Temporal Stability of Gait in Parkinson's Disease. En: *Physical Therapy* 76 (1996)

[36] Meg E. Morris, Jennifer McGinleya Karen D. ; Iansek, Robert: The biomechanics and motor control of gait in Parkinson disease. En: *Clinical Biomechanics* 16 (2001), p. 459–470

[37] Michell, A. W. ; Lewis, S. J. G. ; Foltynie, T. ; Barker, R. A.: Biomarkers and Parkinson's disease. En: *Brain* (2004), p. 1693–1705

[38] Mittal, A. ; Paragios, N.: Motion-based background subtraction using adaptive kernel density estimation. En: *Computer Vision and Pattern Recognition, 2004. CVPR 2004. Proceedings of the 2004 IEEE Computer Society Conference on* Vol. 2, 2004. – ISSN 1063–6919, p. II–302 – II–309 Vol.2

[39] Moeslund, Thomas B. ; Granum, Erik: A Survey of Computer Vision-Based Human Motion Capture. En: *Computer Vision and Image Understanding* 81 (2001), Nr. 3, p. 231 – 268. – ISSN 1077–3142

[40] Mohr, Daniel ; Zachmann, Gabriel: Silhouette Area Based Similarity Measure for Template Matching in Constant Time. En: *ARTICULATED MOTION AND DEFORMABLE OBJECTS* 6169 (2010), p. 43–54. ISBN 978–3–642–14060–0

[41] Nigar Sen Koktas, Gunes Y.: Ensemble Classifiers for Medical Diagnosis of Knee Osteoarthritis Using Gait Data. En: *International Conference on Machine Learning and Applications*, 2006

[42] Nussbaum, Robert L. ; Ellis, Christopher E.: Alzheimer's Disease and Parkinson's Disease. En: *New England Journal of Medicine* 348 (2003), Nr. 14, p. 1356–1364

[43] Pahwa, Rajesh ; Lyons, Kelly E. ; Roller, William C.: *Handbook of Parkinson's Disease*. Marcel Dekker, Inc, 2003

[44] Patrick O. Riley, Kate W. P. ; Kerrigan, D. C.: Eldercare Technology for Clinical Practitioners. (2008), p. 33–51

[45] Piccardi, M.: Background subtraction techniques: a review. 4 (2004), oct., p. 3099 – 3104 vol.4. – ISSN 1062–922X

[46] Poewe, Werner ; Mahlknecht, Philipp: The clinical progression of Parkinson's disease. En: *Parkinsonism & Related Disorders* 15, Supplement 4 (2009), Nr. 0, p. S28 – S32. – ISSN 1353–8020

[47] Profitt, Barton: *Background Subtraction Algorithms for a Video based System*, Stellenbosch University, Tesis de Grado, 2009

[48] Ramaker, Claudia ; Marinus, Johan ; Stiggelbout, Anne M. ; van Hilten, Bob J.: Systematic evaluation of rating scales for impairment and disability in Parkinson's disease. En: *Movement Disorders* 17 (2002), Nr. 5, p. 867–876. – ISSN 1531–8257

[49] Rosenkranz, Bernd. *Biomarkers and Surrogate Endpoints in Clinical Drug Development*. Applied Clinical Trials. 2003

[50] Samii, Ali ; Nutt, John G. ; Ransom, Bruce R.: Parkinson's disease. En: *The Lancet* 363 (2004), Nr. 9423, p. 1783 – 1793. – ISSN 0140–6736

[51] Sofuwa, Olumide ; Nieuwboer, Alice ; Desloovere, Kaat ; Willems, Anne-Marie ; Chavret, Fabienne ; Jonkers, Ilse: Quantitative Gait Analysis in Parkinson's Disease: Comparison With a Healthy Control Group. En: *Archives of Physical Medicine and Rehabilitation* 86 (2005), Nr. 5, p. 1007 – 1013. – ISSN 0003–9993

[52] Stagni, Rita ; Leardini, Alberto ; Cappozzo, Aurelio ; Benedetti, Maria G. ; Cappello, Angelo: Effects of hip joint centre mislocation on gait analysis results. En: *Journal of Biomechanics* 33 (2000), Nr. 11, p. 1479 – 1487. – ISSN 0021–9290

[53] Sutherland, D. H.: The evolution of clinical gait analysis: Part II Kinematics. En: *Gait & Posture* 16 (2002), Nr. 2, p. 159 – 179. – ISSN 0966–6362

[54] Sutherland, David H.: The evolution of clinical gait analysis part l: kinesiological EMG. En: *Gait & Posture* 14 (2001), Nr. 1, p. 61 – 70. – ISSN 0966–6362

[55] Viola, Paul ; Jones, Michael: Robust Real-time Object Detection. En: *International Journal of Computer Vision* (2001)

[56] White, R. ; Agouris, I. ; Fletcher, E.: Harmonic analysis of force platform data in normal and cerebral palsy gait. En: *Clinical Biomechanics* 20 (2005), Nr. 5, p. 508 – 516. – ISSN 0268–0033

[57] Wolf, Sebastian ; Loose, Tobias ; Schablowski, Matthias ; Doederlein, Leonhard ; Rupp, Ruediger ; Gerner, Hans J. ; Bretthauer, Georg ; Mikut, Ralf: Automated feature assessment in instrumented gait analysis. En: *Gait & Posture* 23 (2006), Nr. 3, p. 331 – 338. – ISSN 0966–6362

[58] Wren, C. ; Azarbayejani, A. ; Darrell, T. ; Pentland, A.: Pfinder: real-time tracking of the human body. En: *Automatic Face and Gesture Recognition, 1996., Proceedings of the Second International Conference on*, 1996, p. 51 –56

[59] In: Zhou, Huiyu ; Hu, Huosheng: *Human motion tracking for rehabilitation-A survey*. 2008, p. 1 – 18. ISSN 1746–8094